MICROSTRIP TRANSMISSION LINE THEORY, CHARACTERISTICS, AND COMPONENTS

by

MOHAMED A. USTA

B.Sc. (Electrical Engineering),
University of Libya, 1969

A MASTER'S REPORT

submitted in partial fulfillment of the

requirements for the degree

MASTER OF SCIENCE

Department of Electrical Engineering

KANSAS STATE UNIVERSITY
Manhattan, Kansas

1972

Approved by:

gary johnson
Major Professor

CHAPTER I

INTRODUCTION

The major types of transmission structures which have been utilized in microwave systems are waveguides, coaxial lines, strip lines, and microstrip. Waveguides have comparatively low losses and provide complete shielding, and hence high Q. Coupling between waveguides to form waveguide components is relatively easy. Transmission in waveguides is very well understood and easy to analyze. On the other hand, waveguides have some disadvantages. They are heavy, bulky, dimensionally critical, and expensive. Coaxial lines have a simple and well understood transmission mode. Coaxial components can be made smaller than waveguides for a given wavelength, but usually require critical tolerances that make them still more expensive.

In an attempt to reduce the cost, strip transmission line was introduced in the late forties. It is a flattened coaxial line with the sides removed, or it is a parallel plate waveguide with addition of a strip conductor between the plates. Figure 1.1 shows the configuration of the strip transmission line. While yielding a configuration that is somewhat simpler to fabricate, strip line still requires that close tolerances be maintained as in the case of coaxial construction.

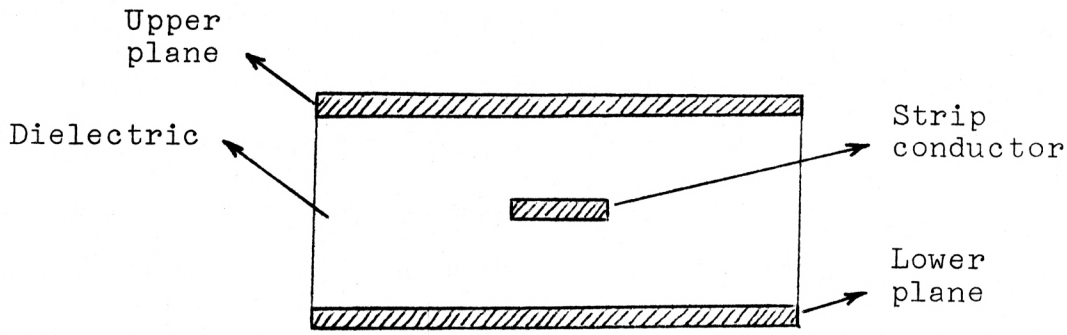

Fig. 1.1. Strip transmission line.

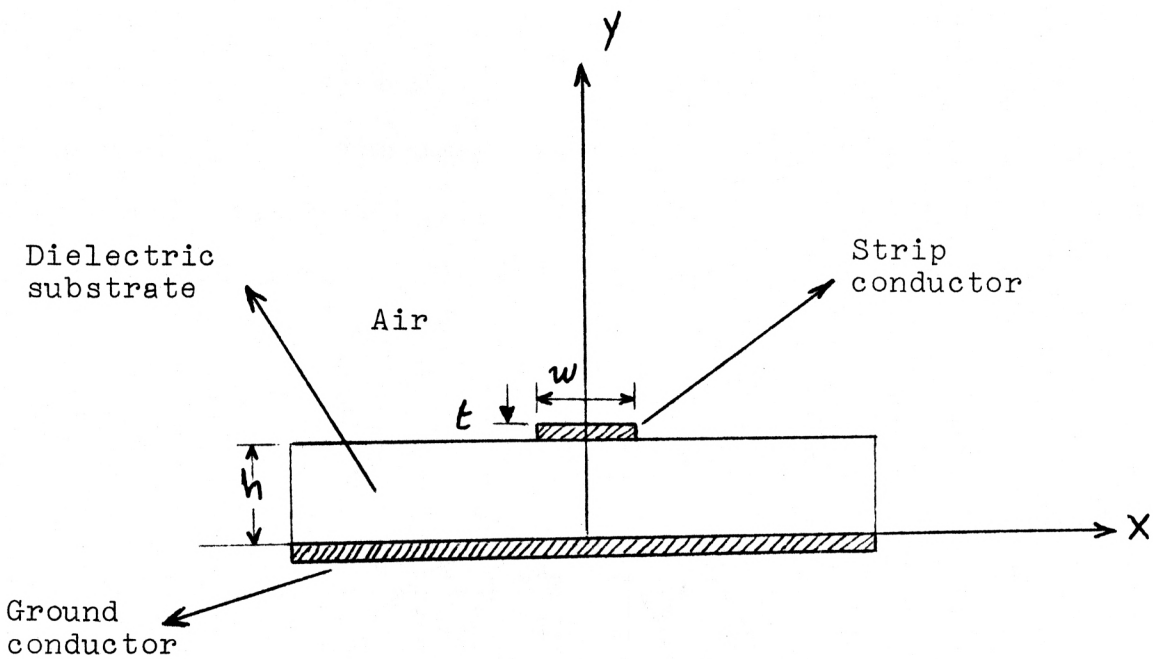

Fig. 1.2. Microstrip transmission line.

In 1952, microstrip as a novel approach to microwave transmission was described (1). It was reported (1, 2, 3) that microstrip losses are approximately equal to those of coaxial structures and microstrip components are nearly as good as waveguide and coaxial components. It was also reported that printed circuit techniques are applicable to the construction of compact, rugged, inexpensive, and noncritical microwave components in microstrip form. Since then microstrip has been under serious study and investigation. The microstrip configuration is shown in Fig. 1.2. It is a thin strip of copper, aluminum, silver, or gold bonded to a slab of dielectric, called a substrate, on which a ground plane, usually of the same metal as the strip, is printed. The strip and ground are the two conductors of microstrip.

The microstrip configuration is equivalent to a parallel wire system since the image of the strip conductor in the ground plane produces the required symmetry. Figure 1.3 shows the electric and magnetic field configuration of microstrip.

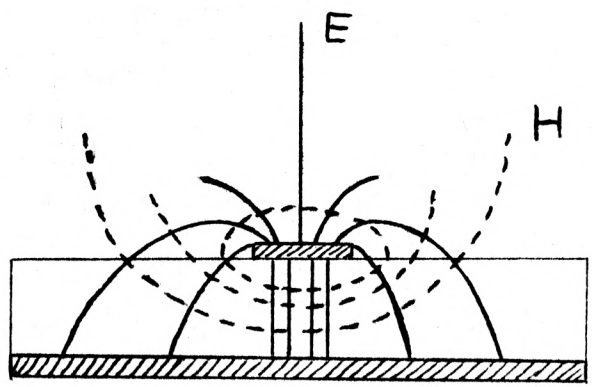

Fig. 1.3. Microstrip field configuration. Solid lines represent the electric field and dotted lines represent the magnetic field.

Despite the physical simplicity of the microstrip transmission line, the rigorous mathematical analysis of its properties presents considerable difficulties. When the microstrip conductors are embedded in a homogeneous isotropic dielectric medium of infinite extent, it is possible to assume uniform propagation in the TEM mode provided that certain critical dimensions do not exceed an appreciable fraction of a wavelength (6). This reduces the problem to a two-dimensional analysis of the static field between parallel plates, i.e., solving Laplace's equation $\nabla^2 \Psi = 0$.

Since the conductor is not embedded totally in the dielectric, one cannot expect pure TEM mode propagation along the line and a more complex mode of propagation is instead expected to exist. That is, since the velocity of propagation in the dielectric is different from that in air, no TEM mode is possible in this structure. In fact, even pure TE or TM modes are not possible (7). If the strip is narrow and the dielectric substrate is thin, then the electric and magnetic fields may be considered separately. The major part of the magnetic field is set up by the axial z component I_z of the current density on the strip (Fig. 1.2).

Since the dielectric is nonmagnetic, it has no effect on the magnetic field. The electric field is set up by the charge density q, and the solution of an electrostatic problem gives the approximate distribution of charge density. Once I_z and q are known, the transverse x-component I_x of the current density may be found by the equation of continuity. Since the I_z and q

distributions are necessarily different, I_x is never identically zero.

Among the researchers who have studied the problem, M. Schetzen in his Master's thesis (MIT, 1954) assumed I_x to be zero since it is approximately proportional to the small width of the strip. Dukes (6) reported an experimental method using an electrolytic tank for studying the microstrip line. Wu in his theory (7) avoided any assumption in order to come up with a complete rigorous solution to this problem. He proposed a set of dual integral equations for the two current components on the strip and presented an iterative solution to the integral equations. Wu's equations are quite complicated and have not been reduced to practical terms, to our knowledge.

Wheeler (9 and 10) theoretically derived a general approximate solution for a similar problem. His basic approximation was to assume TEM mode propagation and to use a conformal mapping technique.

Green and others derived numerical solutions for similar lines. They also assumed TEM mode propagation but mapped the fields by using finite difference approximations of Laplace's equations with an overrelaxation program on a digital computer.

A variational method for the analysis of microstrip lines has been presented by Yamashita and Mitra (17) based on Fourier transform and variational techniques. They employed the concept of capacitance of the line to calculate the characteristic impedance, guide wavelength, and the surface potential on the dielectric sheet of the microstrip.

Bryant and Weiss (21) introduced a solution of the microstrip problem in the "quasi-static" limit; i.e., for the frequency range in which propagation may be regarded as approximately TEM. Such a solution is valid, as they proved, in the range extending into the low gigahertz region, in the case of microstrip dimensions and substrate materials frequently used in integrated microwave circuit technology. This method involves the determination of a "dielectric Green's function" which characterizes the effect on the field configuration due to the presence of the dielectric-air interface.

When the finite difference technique was applied to the solution of coupled-line parameters for microstrip, the computation time became prohibitively long. Judd, Clowes, and Rickard (23) described an analytical method for calculating such parameters with the assumption of TEM propagation. They discovered experimentally that the phase velocity for 50-ohm lines deviates by some three per cent from the theoretical value, assuming pure TEM mode propagation at 10 GHz, with the deviation at lower frequencies being less.

It turns out that the experimental data are in good agreement with Wheeler's theoretical results, that is, the assumption of TEM mode propagation is a very good approximation (15).

The report will deal only with microstrip lines and components printed on nonmagnetic substrates. Most of these lines and components are unshielded.

CHAPTER II

THEORY OF MICROSTRIP TRANSMISSION LINE

2.1. General Theory

Wheeler's calculations are actually for the parallel strip line, Fig. 2.1, which with a simple transformation yields results applicable to microstrip.

Referring to Figs. 1.2 and 2.1, if w = 2a and h = b, then the wavelength of the parallel plane guide shown in Fig. 2.1 is equal to that of the microstrip shown in Fig. 1.2, and the impedance of the microstrip is one-half the impedance of the parallel plane guide. Using this procedure one could analyze the microstrip and come up with fairly accurate results, including (w/h) less than unity and impedances around 50 ohms. Coulton, Hughes and Sobol (12) applied the above transformations to Wheeler's results and came up with quite useful curves for Z_o, the characteristic impedance of the microstrip, and the wavelength λ normalized to that of a microstrip completely embedded in a dielectric (λ_{TEM}), as shown in Fig. 2.2, both as a function of the microstrip width to dielectric thickness ratio (w/h).

These Z_o versus (w/h) curves are given in Fig. 2.3. The characteristic impedance decreases by about a factor of ten as (w/h) increases by a factor of 100. These curves, Fig. 2.3, are very important as design curves since by knowing (w/h) and the

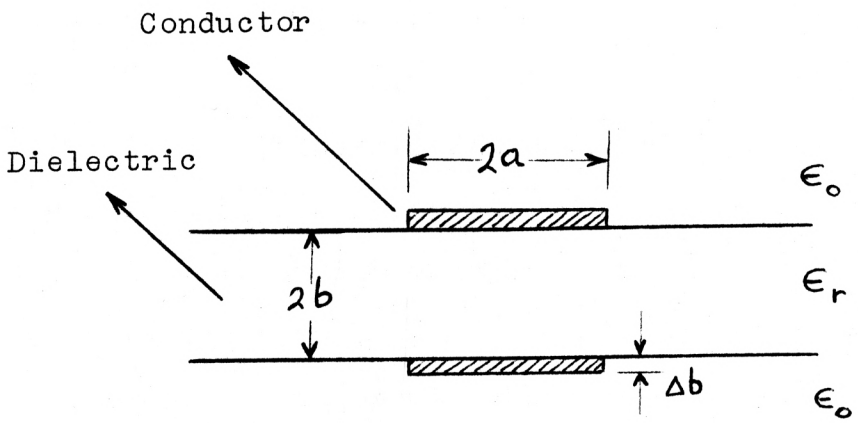

Fig. 2.1. Parallel plane guide.

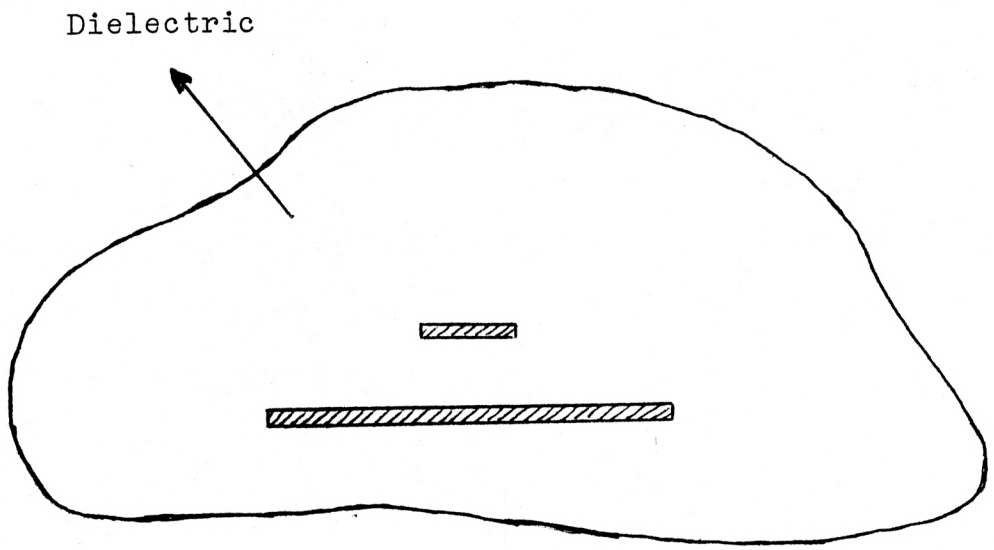

Fig. 2.2. Microstrip embedded in dielectric for calculation of λ_{TEM}.

dielectric constant of the substrate, the characteristic impedance of the microstrip can be obtained. It is about 50 ohms for $(w/h) = 1$ and $\epsilon_r = 10$.

Figure 2.4 shows the (λ/λ_{TEM}) versus (w/h). From these curves λ of the microstrip can be obtained. For example, for $(w/h) = 1$ and $\epsilon_r = 10$, the ratio of λ to λ_{TEM} is about 1.23, and since λ_{TEM} is easily calculated, λ of the microstrip can be easily obtained.

The finite thickness of the line (t) has an effect on the line capacitance. An approximate correction can be made by assuming an effective width w_e.

$$w_e = w + \Delta w \quad . \tag{2.1}$$

Δw is an incremental width given by

$$\Delta w = \frac{t}{\pi} \left(\ell n \frac{2h}{t} + 1 \right) \tag{2.2}$$

This equation is derived from Wheeler's equation for the case of a parallel plane guide, by putting $\Delta w = 2\Delta a$, $h = b$, and $\Delta b = t$. Wheeler's equation is

$$\Delta a = \frac{\Delta b}{2\pi} \left(\ell n \frac{2b}{\Delta b} + 1 \right)^* \quad . \tag{2.3}$$

---

*Pucel, Masse', and Hartwig in their important paper (18) misinterpret this equation, and hence they came up with a different equation for Δw. In their equation

$$\Delta w = \frac{t}{\pi} \ell n \left(\frac{2h}{t} + 1 \right)$$

where the left parenthesis has been misplaced.

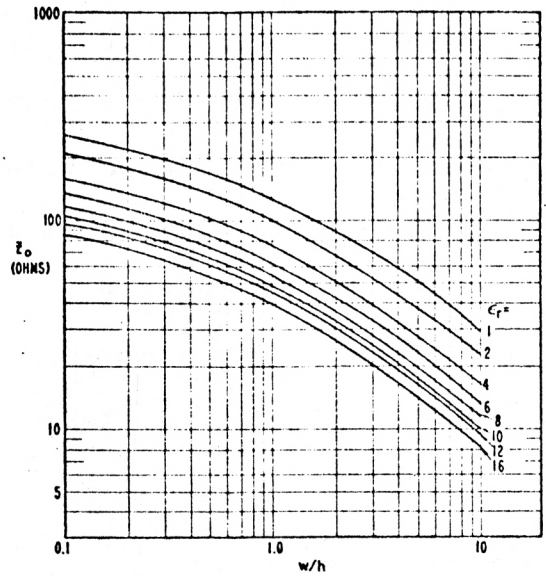

Fig. 2.3. Calculated characteristic impedance Z_o of microstrip lines as a function of w/h and ϵ_r.

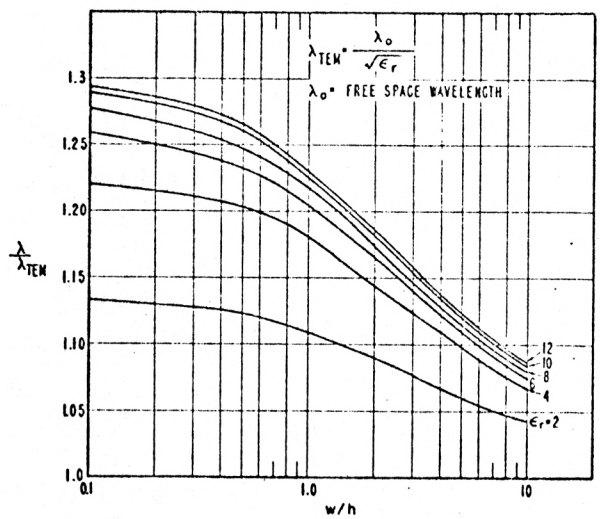

Fig. 2.4. Calculated normalized wavelength as a function of w/h and ϵ_r.

The value of the correction ($\Delta w/t$) is plotted for various (h/t) ratios in Fig. 2.5. The effective width should be used when applying the design curves. Wheeler cautions the reader regarding the effectiveness of this edge correction for high dielectric constant media, since $\Delta w \rightarrow 0$ for $\epsilon >> \epsilon_0$. Therefore equation (2.2) should be regarded as a limit correction for lines where the fringe fields make up an appreciable part of the total fields, a condition that applies for most of the lines in use today.

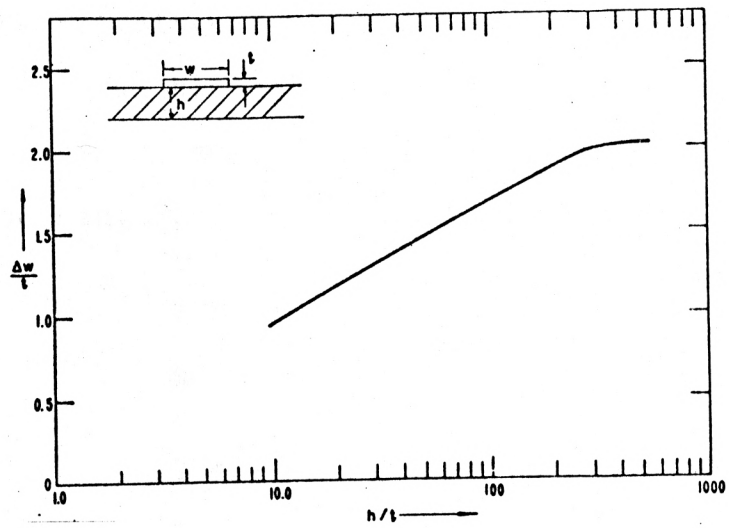

Fig. 2.5. Line width correction for finite thickness substrates.

The quality factor, Q, of the microstrip is best understood by considering a ($\lambda/4$) shorted resonator, to estimate the performance of microstrip in circuit applications. The unloaded Q_u of the resonator can be expressed as

$$\frac{1}{Q_u} = \frac{1}{Q_c} + \frac{1}{Q_d} \qquad (2.4)$$

where Q_d is the quality factor of the dielectric and Q_c is that of the conductors.

If the strip conductor and the ground are made from the same material, which is usually the case, Q_c may be expressed as (12):

$$Q_c = \frac{\omega_o Z_o^2 C}{r_t} \tag{2.5}$$

where ω_o = the resonant frequency

Z_o = the characteristic impedance

C = the capacitance per unit length

r_t = the total series conductor loss per unit length.

Let Q_c be expressed in normalized form in order to use the data of Fig. 2.3 and Fig. 2.4. Substitute in equation (2.5) for ω, C, and r_t as follows:

$$\omega_o = 2\pi f_o$$

$$C = \frac{1}{Z_o v}$$

where v is the velocity of propagation.

$$r_t = \frac{2R_s}{w}$$

R_s is the surface resistivity of both strip and ground conductors. Equation (2.5) becomes:

$$Q_c = \frac{\pi w Z_o \sqrt{\sigma_c}}{\lambda \sqrt{\pi \mu f}} .$$

By multiplying numerator and denominator by $\sqrt{f}$ and putting

$$f = \frac{1}{\lambda_{TEM}\sqrt{\mu\epsilon}} \quad ,$$

then

$$Q_c = wZ_o\sqrt{\pi\sigma_e}\ (\frac{\lambda_{TEM}}{\lambda})\sqrt{\epsilon f} \ .$$

Now put $\epsilon = \epsilon_o\ \epsilon_r$:

$$Q_c = wZ_o\sqrt{f\sigma_c}\ \ (\frac{\lambda_{TEM}}{\lambda})\sqrt{\pi\epsilon_o}\sqrt{\epsilon_r} \ .$$

Put $$\epsilon_o = \frac{1}{36\pi}\ 10^{-9}$$

$$Q_c = (\frac{\lambda_{TEM}}{\lambda})\ w\ Z_o\sqrt{f\sigma_c}\ (\frac{10^{-3}}{6})\ \sqrt{\epsilon_r} \ .$$

Therefore Q_c may be put in the form:

$$\frac{6\ Q_c}{h\sqrt{\sigma_c}}\ \ \frac{10^3}{\sqrt{f}} = (\frac{w}{h})\ (\frac{\lambda_{TEM}}{\lambda})\ Z_o\sqrt{\epsilon_r} \ .$$

Or if f is in GHz this equation becomes:

$$\frac{6\ Q_c}{h\sqrt{\sigma_c}}\ \ \frac{1}{\sqrt{f}} = (\frac{w}{h})\ (\frac{\lambda_{TEM}}{\lambda})\ Z_o\sqrt{\epsilon_r} \ . \qquad (2.6)$$

The left-hand side of equation (2.6) is plotted against the microstrip geometry (w/h) in Fig. 2.6).

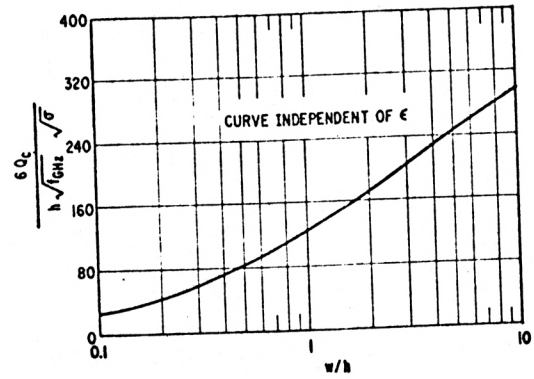

Fig. 2.6. Calculated normalized Q_c as function of (w/h) (MKS units).

The dielectric quality factor Q_d is the ordinary Q value of the material used. It is given by:

$$Q_d = \frac{\omega \epsilon'}{\sigma + \omega \epsilon''}$$

where $\hat{\epsilon}(\omega) = \epsilon' - j\epsilon''$.

The theory described above is a general one and the design data mentioned apply to microstrip in general except when a completely different dielectric material is used, such as an anisotropic material.

2.2. Losses in Microstrip

The topic of losses in microstrip has not received much attention since Assadourian and Rimai (2) derived expressions for conductor and dielectric losses.

Dukes (6), among other authors, has noted that the losses predicted by Assadourian and Rimai are higher than those actually observed.

Pucel, Masse', and Hartwig (18) proposed approximate expressions for the conductor losses covering a wide range of geometrical parameters and applicable to the microstrip on a dielectric substrate. They compared their theory with data taken on rutile and alumina microstrip and obtained good agreement. This theory, which is based on Wheeler's "incremental inductance rule", predicts conductor losses considerably lower than the other theories and apparently has the best agreement with experimental data.

Pucel's loss theory starts with the consideration of only nonmagnetic dielectric substrates to get just two types of loss in the dominant microstrip mode, namely, dielectric losses in the substrate and ohmic skin losses in the strip conductor and the ground plane. Therefore the total attenuation α is given by:

$$\alpha = \alpha_{c1} + \alpha_{c2} + \alpha_d \tag{2.7}$$

where α_{c1} is the attenuation in the strip conductor

α_{c2} is the attenuation in the ground plane

α_d is the dielectric attenuation.

These losses are represented in terms of an attenuation factor α in the expression for the transmitted power P(z) which is the power at any point z along the line. It is given by

$$P(z) = P_o e^{-2\alpha z} \tag{2.8}$$

where z is the direction of propagation parallel to the strip conductor and P_o is the transmitted power at an earlier point

$z = 0$. The total attenuation α is the sum of α_c, the attenuation in the conductors, and α_d.

Differentiate equation (2.8) with respect to z. One obtains

$$\frac{dP(z)}{dz} = -2\alpha P_o e^{-2\alpha z} = -2\alpha P(z) .$$

Therefore

$$\alpha = -\frac{dP}{dz}/2P(z) \approx \frac{P_c + P_d}{2P(z)} \text{ neper/unit length.} \quad (2.9)$$

Then $$\alpha_d \approx \frac{P_d}{2P(z)} \text{ N/unit length} \quad (2.10)$$

and $$\alpha_c \approx \frac{P_c}{2P(z)} \text{ N/unit length} \quad (2.11)$$

where P_d and P_c denote the average dielectric and conductor power losses.

For comparison between dielectrics, it is more meaningful to use the loss per wavelength which can be obtained from equation (2.10) simply by multiplying by the guide wavelength $\lambda_g (\lambda_g = \lambda_o/\sqrt{\epsilon_e})$, where λ_o is the free space wavelength and ϵ_e is the effective dielectric constant of the substrate.

Let the two microstrip losses be treated separately. The dielectric losses will be treated first.

Wheeler (9) stated a relation between a fraction he called the filling factor (q) and the effective dielectric constant of the substrate from the concept of parallel capacitors.

$$q = \frac{\epsilon_e - 1}{\epsilon_r - 1}$$

or

$$\epsilon_e = 1 + q(\epsilon_r - 1) \ . \qquad (2.12)$$

If q = 1, which is the case for other systems, the effective dielectric constant ϵ_e given by equation (2.12) is like that of the substrate ϵ_r, and since q is a fraction ϵ_e of microstrip is always less than ϵ_r. The effective dielectric constant of microstrip will be considered in more detail later.

Following the approach of Wheeler in determining the filling factor for the dielectric constant, Pucel, Masse', and Hartwig (18) derived an expression for the dielectric loss in terms of (q) and the loss tangent tan δ (tan $\delta = \frac{\sigma}{\omega\epsilon}$) on the assumption of air as the upper dielectric.

$$\alpha_d \approx 27.3 \left(\frac{q\epsilon_r}{\epsilon_e}\right) \frac{\tan \delta}{\lambda_g} \quad \text{dB/cm}$$

or (2.13)

$$\alpha_d \approx 4.34 \frac{q}{\sqrt{\epsilon_e}} \sqrt{\frac{\mu_o}{\epsilon_o}}\, \sigma \quad \text{dB/cm}$$

where σ is the conductivity, ϵ_r is the dielectric constant of the substrate, λ_g is the microstrip wavelength ($\lambda_g = \lambda_o/\sqrt{\epsilon_e}$), and ϵ_e is the effective dielectric constant given by equation (2.12).

Equations (2.13) apply only if the loss tangent of the dielectric above the microstrip, in this case air, is equal to the loss tangent of the dielectric substrate. In fact, equating

the tangents is necessary to apply Wheeler's filling factor approach. For a low loss dielectric, however, tan $\delta << 1$ and the assumption of a lossless upper dielectric (air) introduces a negligible error.

Figure 2.7 illustrates the dependence of the dielectric filling factor q, multiplied by the ratio (ϵ_r/ϵ_e) for convenience, on the geometry of the microstrip as given by Pucel (18) for a range of dielectric constants suitable for microwave integrated circuits (MIC).

Pucel also plotted against (w/h) the product $\alpha_d \rho$, where ρ is the reciprocal of σ, for two semiconducting substrates which are being used for MIC technology, namely, silicon and gallium arsenide. Figure 2.8 shows these two curves. Silicon (k = 11.7) has a higher dielectric loss for the same (w/h).

Sobol (13) proved experimentally that the dielectric loss can be neglected for hybrid IC's on ceramic substrates because conductor losses predominate. When the substrate is a semiconductor, the substrate losses are not negligible. Sobol approximated empirically the losses for semiconductors by:

$$\alpha_d \text{ (semiconductor)} \approx \frac{1}{2} \frac{Z_o w}{\rho_h}$$

$$= \frac{188}{\sqrt{\epsilon_r}\rho} \frac{1}{1 + 1.735 (\epsilon_r)^{-0.0724} (w/h)^{-0.836}}$$

nepers/meter (2.14)

Sobol also calculated and tabulated the losses of the microstrip on ceramic and silicon substrate. Table 2.1 shows his

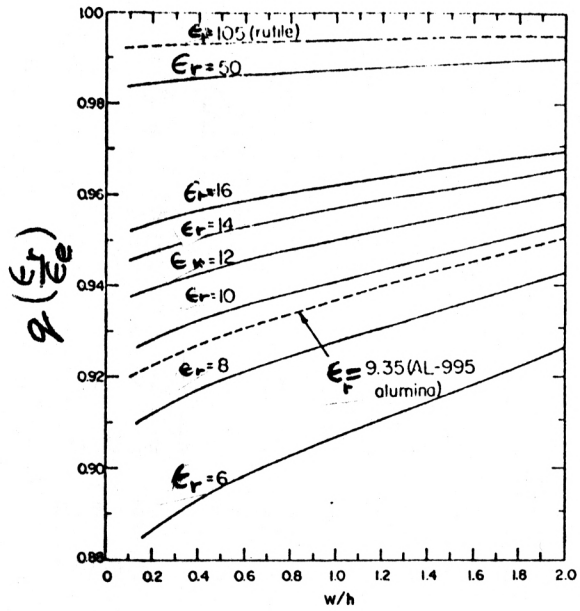

Fig. 2.7. Filling factor for loss tangent of microstrip substrate as a function of w/h.

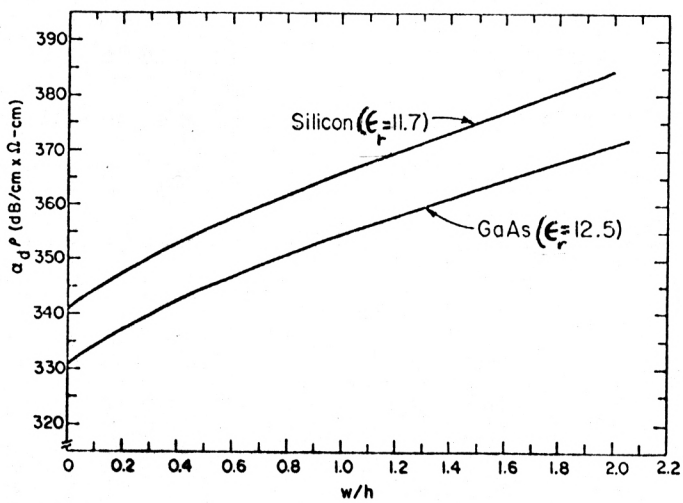

Fig. 2.8. Dielectric attenuation factor of microstrip as a function of w/h for silicon and gallium arsenide substrates.

Table 2.1. Losses of 50-ohm microstrip lines in microwave integrated circuits.

Line	Conductor	Dielectric		ϵ_r	Losses, db/cm		Q of $\lambda/4$ Resonator	
		Material	Thickness		2 Ghz	10 Ghz	2 Ghz	10 Ghz
A	gold	ceramic	10 mils	9.9	0.098	0.22	48	106
B	gold	ceramic	25 mils	9.9	0.039	0.088	120	265
C	gold	silicon (150 ohm-cm)	10 mils		1.3	1.44	2	9
D	gold	silicon (1,500 ohm-cm)	10 mils		0.24	0.38	14	50

No dielectric loss in lines A and B; conductor and substrate loss included for lines C and D

calculations. Note that the substrates on lines A and B are assumed to have zero dielectric loss where in substrates C and D the dielectric loss is included because the dielectric is a semiconductor, silicon. The line materials and sizes in the table are typical for microwave integrated circuits. For a gold line on a 10-mil thick ceramic substrate the loss is 0.22 dB/cm at 10 GHz, while the loss is 1.44 dB/cm for the same line on silicon (150 ohm-cm) substrate of the same thickness at the same frequency.

Now that the dielectric losses have been considered, the ohmic losses will be explored. The predominant sources of loss at microwave frequencies are the nonperfect conductors used. The substrate loss is generally negligible.

The ohmic loss factor could be computed from the expression (26):

$$\alpha_c = \frac{R_{s1}}{2Z_o} \int_c \frac{|J_1|^2}{|I|^2}\, dx + \frac{R_{s2}}{2Z_o} \int_c \frac{|J_2|^2}{|I|^2}\, dx \qquad (2.15)$$

This expression comes directly from equation (2.11). R_{s1} is the surface skin resistivity of the strip line and is given by:

$$R_{s1} = \sqrt{\frac{\mu_1 \pi f}{\sigma_1}}$$

R_{s2} is the surface skin resistivity of the ground

$$R_{s2} = \sqrt{\frac{\mu_2 \pi f}{\sigma_2}}$$

$J_1(x)$ and $J_2(x)$ are the corresponding surface current densities. $|I|$ is the magnitude of the total current per conductor. The integration in equation (2.15) should be taken around the surfaces of the conductors, perpendicular to the conductor axis.

Most of the workers have assumed for simplicity that the current distribution is uniform and equal to (I/w) in both conductors. With this assumption the approximate expression for α_c may be obtained from equation (2.15) by integrating from zero to w, putting J = I/w. Therefore α_c is given by:

$$\alpha_c \approx \frac{R_{s1} + R_{s2}}{2Z_o w} \text{ neper/unit length.}$$

Now if the same thick film conductor paste is used, $R_{s1} = R_{s2} = R_s$. Then

$$\alpha_c \approx \frac{R_s}{Z_o w} \text{ neper/unit length}$$

$$= \frac{8.68\ R_s}{Z_o w} \text{ dB/unit length} \qquad (2.16)$$

or

$$\alpha_c \frac{h}{8.68} \cdot \sqrt{\frac{\sigma}{\pi f \mu}} = \left(\frac{1}{Z_o}\right)/(w/h)$$

Coulton (12) plotted the right-hand side of equation (2.16), and therefore also the left-hand side against w/h for different values of ϵ_r, Fig. 2.9. He used the impedance data presented in Fig. 2.3. For (w/h) = 1 and ϵ_r = 10, the left-hand side is equal to about 0.02. Therefore if the conductor is gold and the frequency is 10 GHz, $R_s = 3.12 \times 10^{-7} \sqrt{f} = 0.0312$. Hence for h = 0.03 inch, α_c is about 0.21 dB per inch.

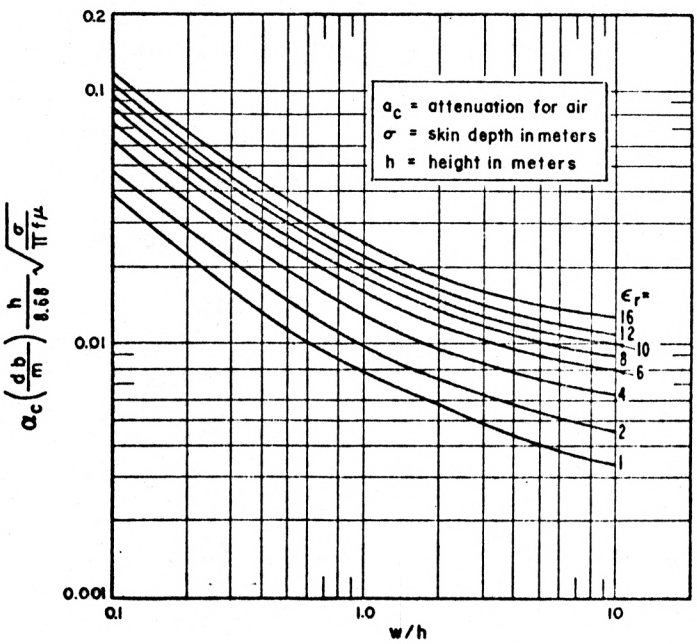

Fig. 2.9. The conductors attenuation as a function of (w/h) for different substrate materials.

Pucel and his colleagues reported that equation (2.16) is valid only for arbitrarily large strip widths (w/h is large). They used another technique for calculating the skin losses, a technique based on the so-called "incremental inductance rule" of Wheeler. This rule, or formula, expresses the series skin resistance R per unit length in terms of that part of the total inductance per unit length which is attributable to the skin effect, that is, to the inductance produced by the magnetic field within the metallic conductors. This technique is based on the assumptions of TEM propagation and the conductors being more than one skin depth thick.

A sketch of the current distribution is shown in Fig. 2.10 for a strip of nonzero thickness t. The strip conductor contributes the major part of the skin loss.

Applying the above mentioned technique, Pucel and the others obtained some expressions for the conductor attenuation. The reader is referred to their work (19) which is a correction to their previous paper (18). Figure 2.11 shows curves of α_c, multiplied by $(Z_o h/R_s)$, against (w/h) for different conductor thicknesses. These curves are based on computations using Pucel's equations of α_c (19). The figure also shows one curve based on equation (2.16) and another based on the Assadorian and Rimai (2) method of computing the conductor losses for microstrip lines printed on alumina and rutile substrates.

This new theory of conductor losses was proved experimentally (18) to give results superior to the other methods developed so far.

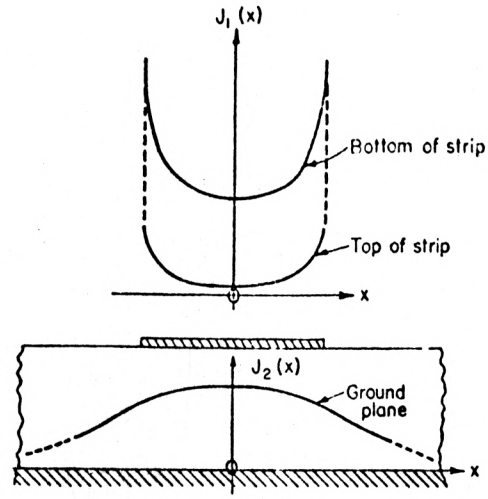

Fig. 2.10. Sketch of the current distribution on microstrip conductors.

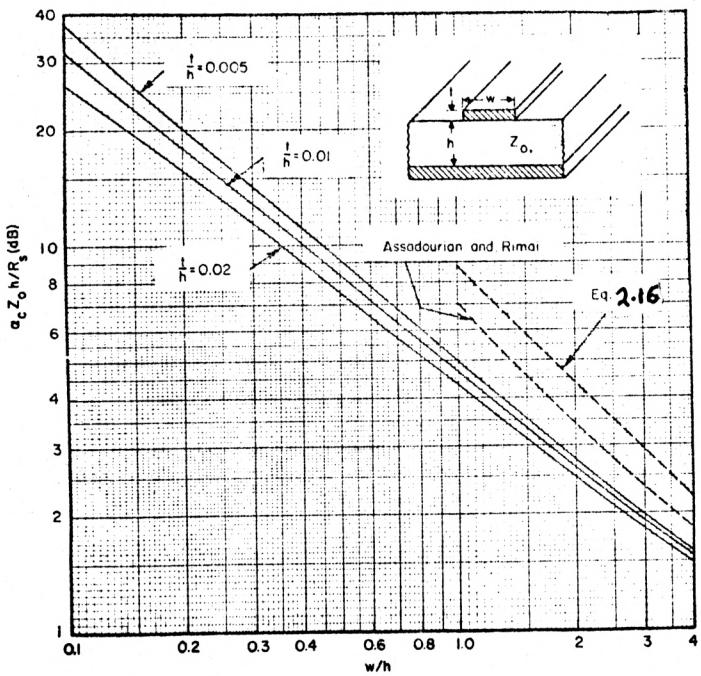

Fig. 2.11. Theoretical conductor attenuation factor of microstrip as a function of w/h.

2.3. Radiation from Microstrip

Any microstrip discontinuity tends to radiate. This brought many difficulties to those working on microstrip resonators. The amount of loss due to radiation might reach 50 per cent of the total insertion loss (18).

Radiation from microstrip in general depends on three factors:

1. Substrate thickness
2. Dielectric constant
3. Microstrip geometry.

In order to arrive at an expression for the radiation resistance, Lewin (see Denlinger, 22), made the following assumptions:

1. TEM transmission.
2. The radiation from the transverse electric field component parallel to the plane of the strip is negligible.
3. The substrate thickness is much less than the free space wavelength λ_o.

Lewin's formula for the radiation resistance R_r of an open circuit can be put in the form using ($K = 2\pi/\lambda$).

$$R_r = 240\ \pi^2\ (\frac{h}{\lambda_o})^2\ F(\epsilon_e) \qquad (2.17)$$

where R_r = radiation resistance in ohms

λ_o = free space wavelength

h = substrate thickness

$F(\epsilon_e)$ = the radiation factor

ϵ_e = the effective dielectric constant,

and

$$F(\epsilon_e) = \frac{\epsilon_e + 1}{\epsilon_e} - \frac{(\epsilon_e - 1)^2}{2\epsilon_e\sqrt{\epsilon_e}} \ln \frac{\sqrt{\epsilon_e} + 1}{\sqrt{\epsilon_e} - 1} \qquad (2.18)$$

Another type of microstrip structure which radiates is the microstrip resonator. There are two types of resonators:

1. Transmission line resonators, made of parallel or series junctions.
2. Disc resonators, involving discs centered in the substrates.

The ratio of the radiation resistance to the characteristic impedance Z_o of microstrip is equal to the fraction of the power radiated from a single open-circuit discontinuity (22). If there are two discontinuities in a transmission line resonator separated by a multiple of half the strip wavelength ($n \frac{\lambda_g}{2}$), then the total radiation will be twice that from one discontinuity (22).

The fraction of the power radiated from the line resonator to the total power delivered can be expressed as:

$$\frac{P_r}{P_t} \propto \left(\frac{h}{\lambda}\right)^2 \frac{F(\epsilon_e)}{Z_o} . \qquad (2.19)$$

The ratio $\left(\frac{P_r}{P_t}\right)$ can be expressed in terms of the quality factor Q (22):

$$\frac{P_r}{P_t} = \frac{Q_o - Q_t}{Q_o} \tag{2.20}$$

where P_r is the power radiated

P_t is the total power delivered

Q_o is the quality factor of the line resonator measured in a long waveguide below cutoff to prevent leakage into space

Q_t is the quality factor measured without any metallic enclosure.

Denlinger derived an empirical formula for (P_r/P_t) from his experimental and theoretical results on a line resonator.

$$\frac{P_r}{P_t} = (5.04 \times 10^4)\left(\frac{h}{\lambda_o}\right)^{1.8} \cdot \frac{F(\epsilon_e)}{Z_o} \tag{2.21}$$

This expression holds only for small values of (h/λ), for which no surface waves will propagate. The following inequality must be satisfied:

$$2\pi \left(\frac{h}{\lambda_o}\right)\sqrt{\epsilon_r - 1} << \frac{\pi}{2}$$

or

$$\left(\frac{h}{\lambda_o}\right)\sqrt{\epsilon_r - 1} << 0.25 \tag{2.22}$$

It is clear from the above discussion that radiation increases with the substrate thickness (h) and decreases with the effective dielectric constant.

Radiation in disc resonators is much greater than in line resonators. Radiation in disc resonators could be reduced by placing a high dielectric constant medium in the immediate vicinity of the edge of the disc (22).

It is apparent that increasing the substrate thickness in order to decrease the insertion loss and improve the power handling capability will be accompanied by an increase in radiation loss. Therefore one should seek the optimum substrate thickness.

2.4. Dispersion in Microstrip

The dispersion phenomenon was discovered since the discovery of the microstrip transmission line. The value of the dielectric constant of the system is not that of the substrate material ϵ_r. The system tends to have an effective dielectric constant given by equation (2.12) which involves a filling factor (q) that depends on several factors such as frequency, effective width of the strip line, characteristic impedance, and ϵ_r.

This topic, dispersive effects in microstrip, has received considerable attention in the literature in recent years (25).

Arnold (see Ref. 25) gave an empirical equation showing the relation between the dispersion and the phase velocity on alumina ($\epsilon_r = 9.9$) substrates for $w/h \leq 2$.

Chudobiak (25) gave an empirical equation describing the variation of ϵ_e, the effective dielectric constant, with frequency for a range of dielectric constants from 2 ($\epsilon_r = 2$) to 10, (w/h) from 0.9 to 13, and substrate thickness from 20 mils to 120 mils. ϵ_e, according to Chudobiak, is given by:

$$\epsilon_e = 3 \times 10^{-6}\, h(\epsilon_r + 1)(\epsilon_r - 1)(f - f_o)\sqrt{Z_o \frac{w_e}{h}} + \epsilon_{eo} \qquad (2.24)$$

when $w/h < 4$,

where ϵ_r = the relative dielectric constant of the substrate

w = the line width in mils

w_e = the effective line width given by equations (2.1) and (2.3)

f = GHz

f_o = frequency below which dispersion may be neglected and given by

$$f_o = \frac{6}{(\epsilon_r - 1)^{1/4}}\sqrt{\frac{Z_o}{h}} \qquad (2.25)$$

and ϵ_{eo} = "Wheeler's effective dielectric constant"* for a given (w/h) and ϵ_r. It is equal to ϵ_e for $f < f_o$.

If $w/h > 4$, equation (2.32) is modified to

$$\epsilon_e = 3 \times 10^{-6}\, h(\epsilon_r + 1)(\epsilon_r - 1)(f - f_o)\left(\frac{w_e}{h}\right)\sqrt{\frac{Z_o}{3}} + \epsilon_{eo} \qquad (2.26)$$

For $\epsilon_r = 10$ and $\frac{w_e}{h} = 1$, ϵ_{eo} is about 7 (see reference 25). Therefore if the frequency is 10 GHz, $w_e = 50$ mils, and $Z_o = 50$ ohms, then f_o is about 3.48 GHz and the effective dielectric constant is about 7.4.

---

*This value is obtainable directly from Wheeler's curves. See "The Microwave Engineers Technical and Buyers Guide," Horizon Press, New York, 1969, pp. 65-66.

CHAPTER III

CHARACTERISTICS OF MICROSTRIP

Microstrip transmission line is characterized by quasi-TEM transmission. It is also characterized by the wavelength, velocity, characteristic impedance Z_o, the quality factor, and the attenuation. The fact that the propagation is complex in nature and not like that of waveguides and coaxial cables was discussed in Chapter I. The attenuation and losses were studied in the last chapter and the difficulty of the current distribution was discussed. Expressions were derived for losses and radiation as well as dispersion.

This chapter is devoted to the study of characteristic impedance, wavelength, and velocity.

Besides its own unique characteristics microstrip has most of the troublesome properties of dispersive waveguide, in that conductor dimensions influence not only characteristic impedance but also the velocity of propagation.

3.1. Characteristic Impedance

The characteristic impedance and the velocity of propagation of a TEM transmission line are given by:

$$Z = \sqrt{L/C} \qquad \text{and} \qquad v = 1/\sqrt{LC}$$

where L and C are the inductance and capacitance of the transmission line per unit length. Substituting for L yields:

$$Z = \frac{1}{vC} . \tag{3.1a}$$

If the dielectric of the line is free space, then

$$Z = Z_o = \frac{1}{cC_o} \tag{3.1b}$$

where c is the velocity of light in free space.

For microstrip transmission line the capacitance C is greater than C_o, the capacitance of the free space transmission line, and the characteristic impedance is given by:

$$Z = \sqrt{\frac{C_o}{C}}\, Z_o \tag{3.2}$$

The new guide wavelength is given by:

$$\lambda_g = \sqrt{\frac{C_o}{C}}\, \lambda_o \tag{3.3}$$

Therefore the basic properties of the microstrip transmission line are derivable from the knowledge of the line capacitance.

Arditi (4) was the first who measured the capacitance C at low frequencies and the velocity of propagation v at microwave frequencies and then used equation (3.2) to find the impedance of dielectric filled microstrip.

Dukes (6) used another approach to calculate the characteristic impedance, namely, the "lower and upper impedance approach". He obtained about the same results as Arditi.

Using the conformal mapping technique, Wheeler obtained a set of curves for the characteristic impedance. Most of Wheeler's curves have been checked experimentally by several workers and appear to be valid. Figure 2.3 shows some curves of Z_o versus (w/h) for different ϵ_r based on Wheeler's theory.

Coulton, Hughes, and Sobol (12) made some experiments on polyguide, sapphire, and lucalox. They obtained results very close to the theoretical results based on Wheeler's theory theory (solid lines). Figure 3.1 shows their experimental results.

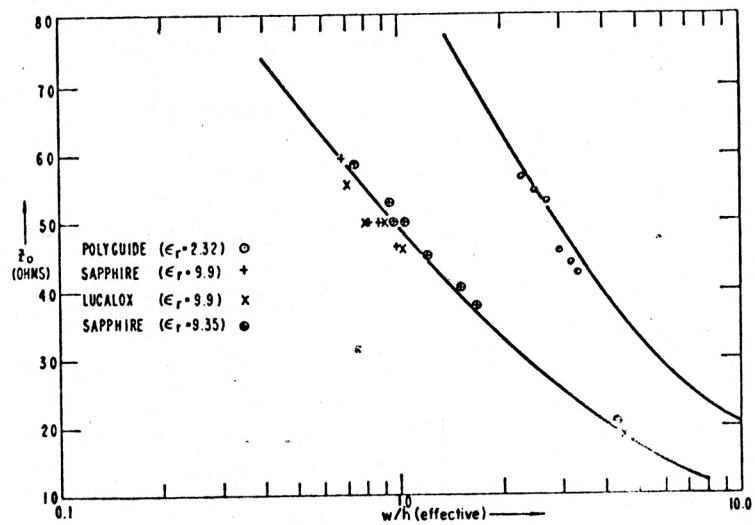

Fig. 3.1. Characteristic impedance Z_o as a function of w/h of microstrip line.

Sobol (13) used Wheeler's curves to obtain empirically the following equation for Z_o of unshielded microstrip transmission line.

$$Z_o = \frac{377\ h}{w\sqrt{\epsilon_r}\left[1 + 1.735(\epsilon_r)^{-0.0724}\ (w/h)^{-0.836}\right]} \qquad (3.4)$$

This equation is accurate to within one per cent for $(w/h) > 0.4$ and $\epsilon_r > 1$, and is even more accurate when $(w/h) > 0.1$.

Equation (3.4) applies when the conductor's thickness is essentially zero. If the thickness is finite, the effective width must be used, as given by equations (2.1) and (2.3).

Vendelin (14) used high dielectric substrates whose dielectric constants range from 25 to 100. He also got good agreement with theory. Figure 3.2 shows his curves. Notice that the high dielectric substrates require smaller values of w/h for high impedance levels because of the higher transmission line capacitance. Since the strip width is restricted by integrated circuit technology limitations, thicker substrates are required for high dielectric microstrip circuits.

Seckelmann (15) presented some further experimental data for impedances and effective dielectric constants. He used alumina substrates for a wide range of parameters. His experimental data agree with Wheeler's analysis. Figure 3.3 shows Seckelmann's results as well as the theoretical curves of Wheeler and Green.

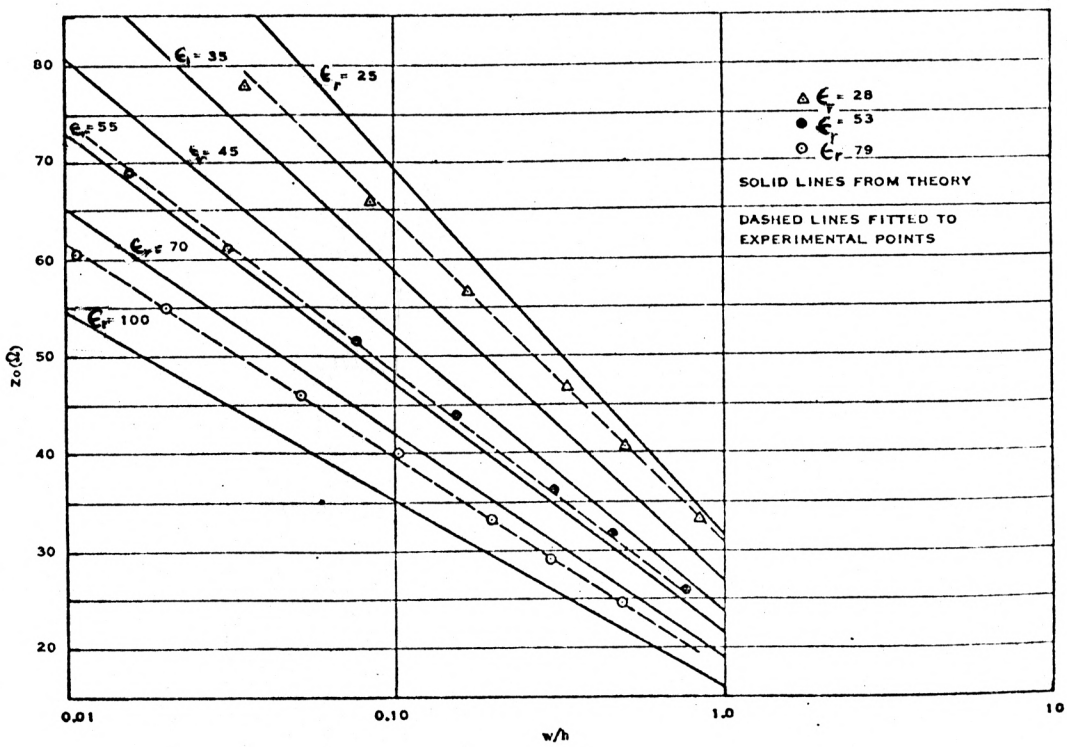

Fig. 3.2. Characteristic impedance of microstrip transmission lines versus dielectric constant and geometry.

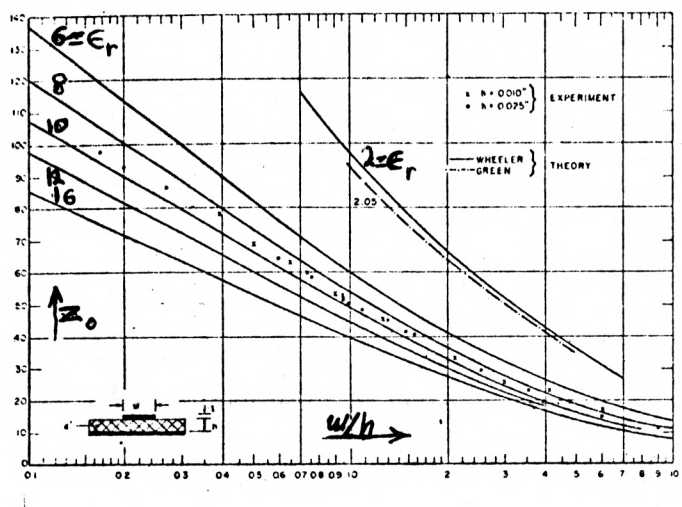

Fig. 3.3. Impedance of microstrip as a function of w/h and ϵ_r.

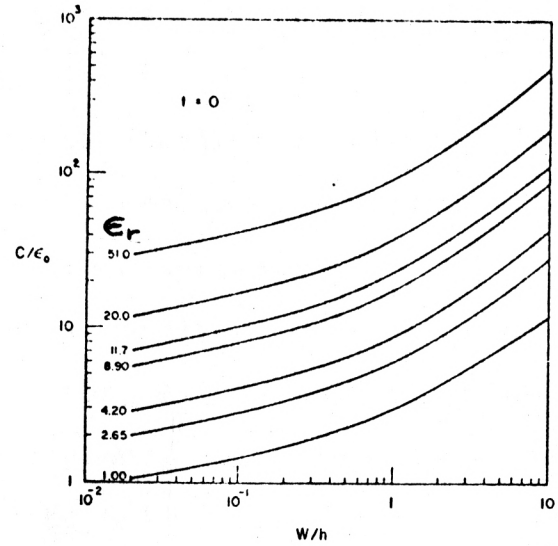

Fig. 3.4. Line capacitance versus strip width and strip height.

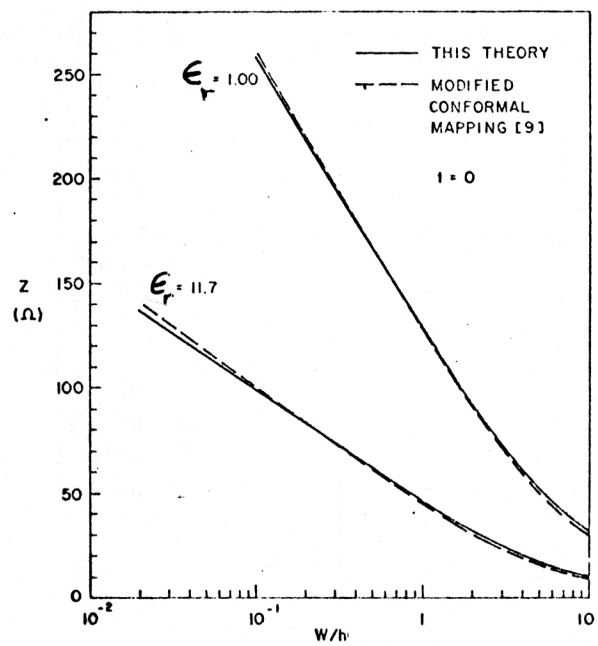

Fig. 3.5. Calculated results for characteristic impedance Z_o and comparison with other theory.

Yamashita and Mitra (17) presented a "variational" method for computing the line capacitance of a microstrip line based on the application of Fourier transforms and variational techniques. Figure 3.4 shows their numerical results for the line capacitance for various parameters.

Figure 3.5 shows their calculated results for characteristic impedance Z_o for $\epsilon_r = 1$ and $\epsilon_r = 11.7$; ϵ_r is the relative dielectric constant, along with those based on the modified conformal mapping technique of Wheeler. Comparison shows that the results obtained by Yamashita and Mitra agree well with Wheeler's theory for both the narrow and wide strips.

Figure 3.6 shows the calculated results for the characteristic impedance for a range of dielectric constants. Yamashita and Mitra's experimental data for Teflon Fiberglas ($\epsilon_r = 2.65$) and Fiberglas G-6 ($\epsilon_r = 4.2$) are also displayed on the figure.

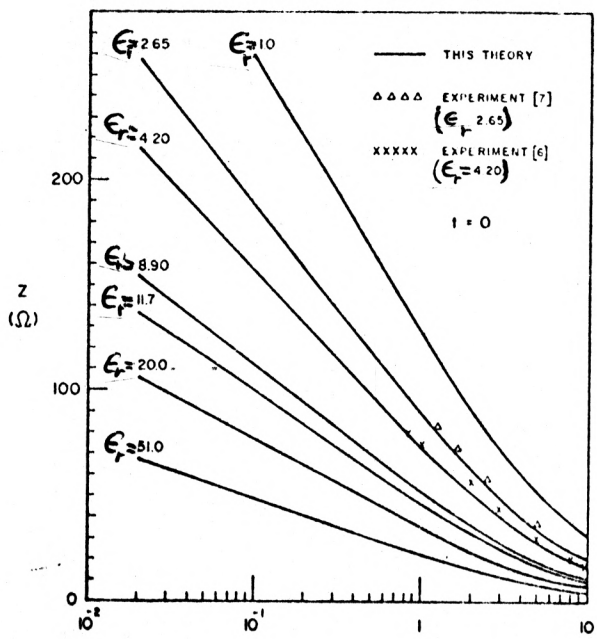

Fig. 3.6. Theoretical and experimental characteristic impedance for various dielectric constants.

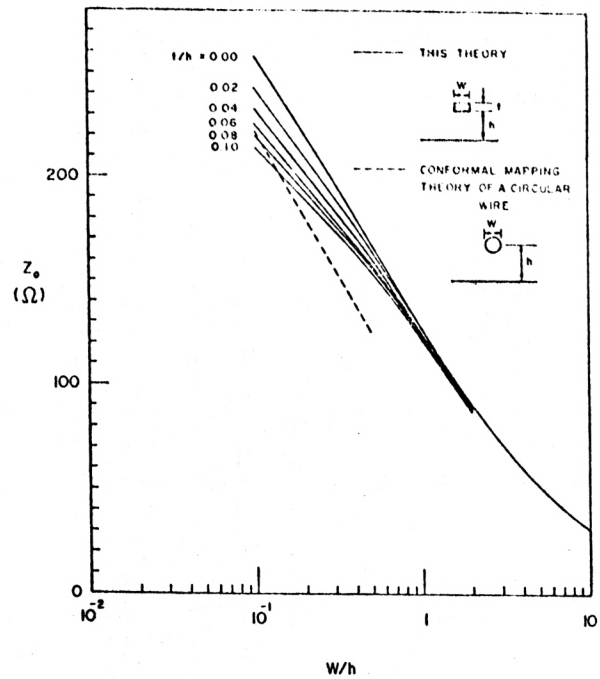

Fig. 3.7. Effect of strip thickness on characteristic impedance with $\epsilon_r = 1.00$.

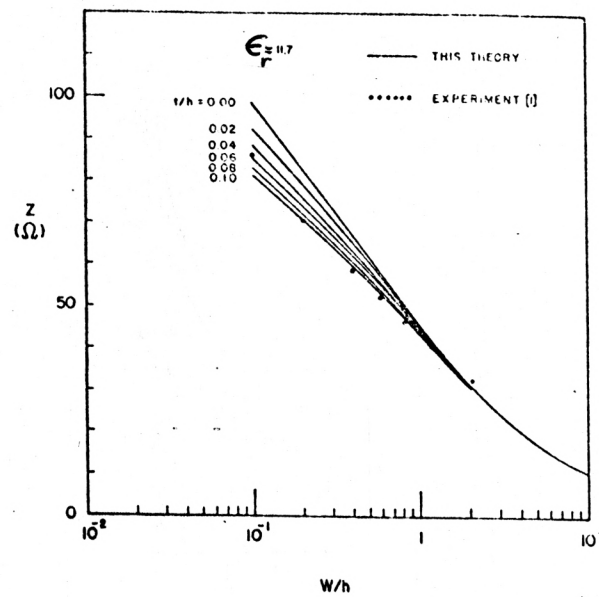

Fig. 3.8. Theoretical and experimental results for the effect of strip thickness on characteristic impedance with $\epsilon_r = 11.7$.

Yamashita and Mitra studied also the effect of the strip thickness (t) on the characteristic impedance. They came to the conclusion that strip thickness does affect the value of the characteristic impedance. Figure 3.7 shows the effect of t upon Z_o for different microstrip geometries for $\epsilon_r = 1$. Figure 3.8 shows the same effect when $\epsilon_r = 11.7$.

Bryant and Weiss (21) presented some curves for the characteristic impedance based on their method. They proved that

$$Z_o = \frac{1}{c\, C_1 \sqrt{\epsilon_e}} \tag{3.5}$$

where C_1 is the capacitance per strip and ϵ_e is the effective dielectric constant. Their curves, showing the characteristic impedance versus (w/h) for various relative dielectric constants, are given in Fig. 3.9.

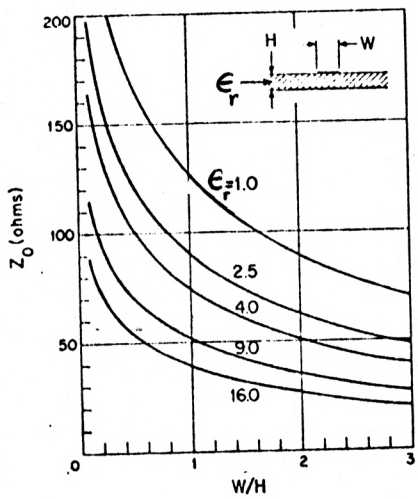

Fig. 3.9. Characteristic impedance of microstrip--single strip.

Judd, Clowes, and Rickard (23) studied the shielded microstrip line (Fig. 3.10) and presented two curves for $\epsilon_r = 9.3$ and $\epsilon_r = 9.8$. Figure 3.11 shows the characteristic impedance of shielded microstrip as it varies with the ratio (w/h) for microstrip on commercially available alumina substrates. Some applications require shielding, which is putting the microstrip system in a metallic enclosure or packaging for hermetic sealing and strength; this will confine the fringe field. Therefore the conducting boundaries, Fig. 3.10, may be regarded as either actual physical boundaries whose object is to limit radiation and coupling to other components, or as convenient mathematical fictions. In the latter case, their distance from the strip conductor can be chosen so that their presence has a negligible effect on the value of the impedance. It has been noted (12) that if the distance from the conductor to the metallic enclosure is several (3 to 5) times the height of the insulating layer, the propagation characteristics are only slightly perturbed.

From Figs. 2.3 and 3.11 it is clear that the characteristic impedance of w/h = 1 and $\epsilon_r = 9.8$ microstrip is slightly lower for the shielded case. The shielding reduces Z_o by about 3 ohms.

3.2. Propagation Wavelength and Velocity

Because of the complexity of the propagation mode it has been found difficult to get exact expressions for λ_g and v, microstrip wavelength and velocity of propagation respectively. Microstrip differs from waveguides and coaxial systems where the nature of propagation is well known, and hence straightforward

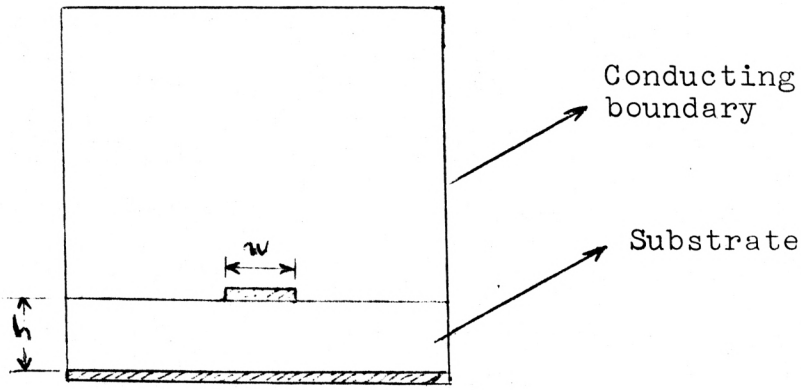

Fig. 3.10. Shielded microstrip.

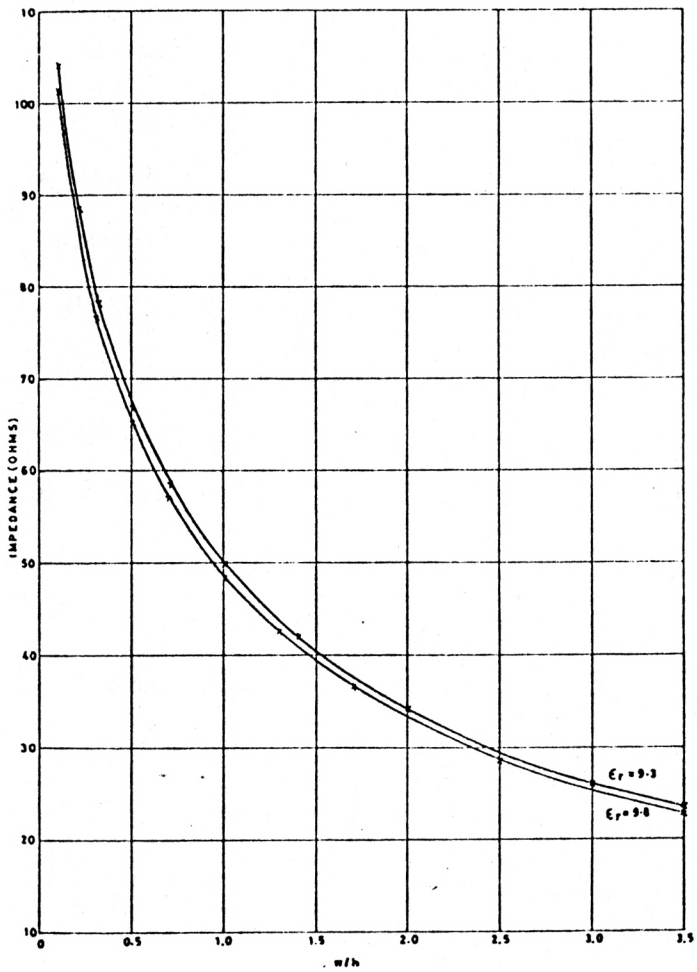

Fig. 3.11. Characteristic impedance of single strip microstrip.

expressions can easily be obtained. It has been found necessary to plot curves for λ_g and v for quick reference.

Propagation Wavelength. Kostriza (3) was the first who studied the microstrip wavelength twenty years ago. He made some experiments on different dielectrics and different thicknesses to obtain some useful curves in the absence of an exact expression for λ_g. Figure 3.12 shows Kostriza's curves from which it is clear that:

1. For air-filled microstrip, $\lambda_g = \lambda_o$.
2. For a given width of line conductor, λ_g decreases as the thickness of the dielectric increases.
3. For a given thickness of dielectric, λ_g decreases as the width of the line conductor increases.
4. For a given thickness of dielectric and strip conductor width, λ_g decreases as the dielectric constant of the material increases.

Coulton, Hughes, and Sobol transformed Wheeler's results on parallel plane guide to microstrip and presented some useful curves shown in Fig. 2.4. They also measured values of λ for typical values of (w/h) on sapphire and Polyguide substrates. Figure 3.13 shows their results (see Fig. 2.5 and the comment on it).

Sobol empirically derived the following equations for λ_g from the experimental curves.

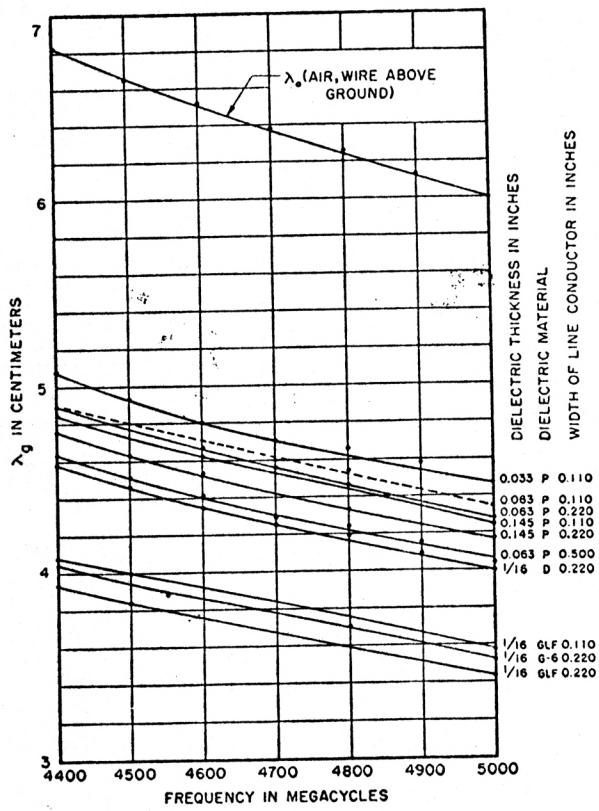

Fig. 3.12. Phase wavelengths plotted vs. frequency. The upper curve is for wire above ground in air. The dielectrics are P = polystyrene, D = Dielecto, G6 = G6 Formica, and GLF = Synthane.

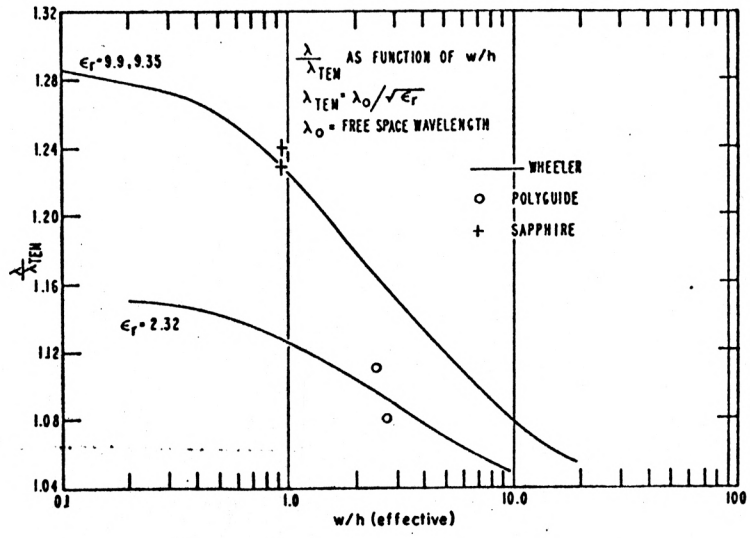

Fig. 3.13. Normalized wavelength as function of w/h of microstrip line.

$$\frac{\lambda_g}{\lambda_{TEM}} = \sqrt{\frac{\epsilon_r}{1 + 0.63(\epsilon_r - 1)(w/h)^{0.1255}}} \quad \text{for } w/h \geqslant 0.6$$

$$\frac{\lambda_g}{\lambda_{TEM}} = \sqrt{\frac{\epsilon_r}{1 + 0.6(\epsilon_r - 1)(w/h)^{0.0297}}} \quad \text{for } w/h \leqslant 0.6 \qquad (3.6)$$

where λ_{TEM} is the wavelength of a microstrip completely embedded in the dielectric.

If the thickness of the conductors is appreciable compared to the dielectric thickness h, the effective width should be used.

In equation (3.6) it is clear that when $\epsilon_r = 1$, that is, when air is used as a dielectric, then the propagation is TEM.

Vendelin (14) used high dielectric substrates to study the microstrip wavelength λ_g. He plotted the measured and calculated ratios of free space wavelength to microstrip wavelength. Figure 3.14 shows his curves which are computed from the conformal

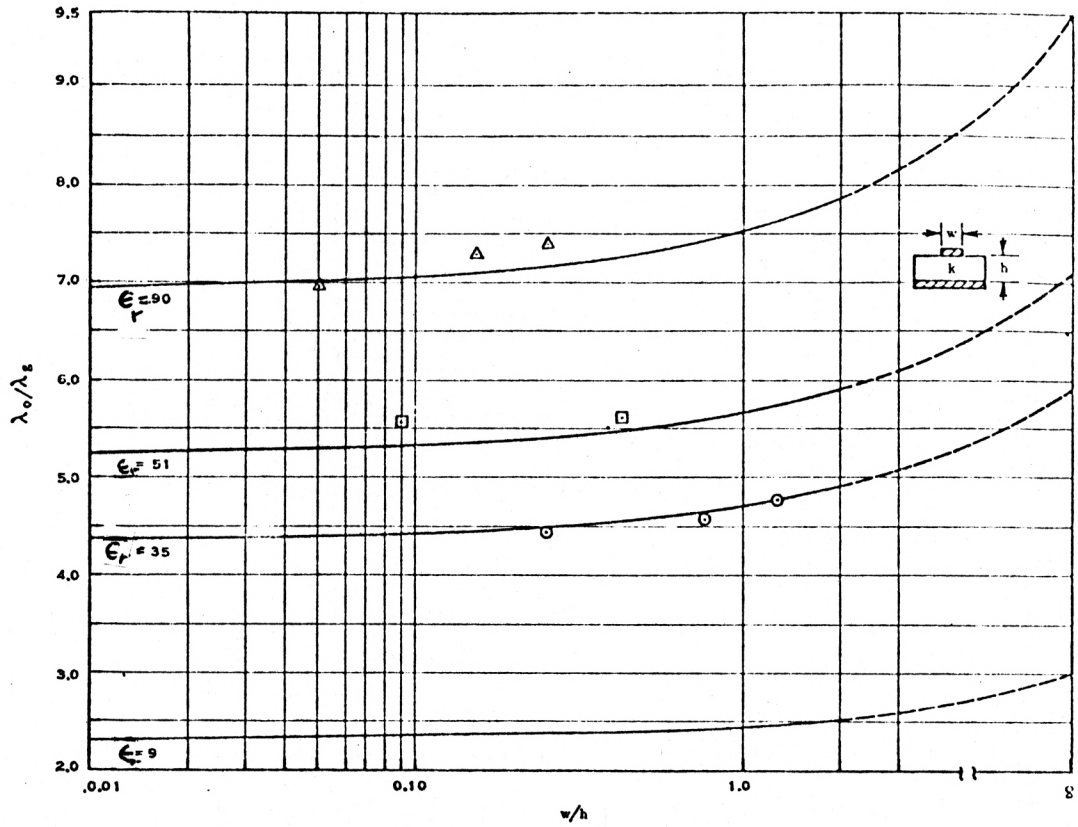

Fig. 3.14. λ_o/λ_g versus dielectric constant and geometry for microstrip transmission lines.

mapping solution. The figure also shows his measurements which are quite close to the theory.

Vendelin's work proves that the conformal mapping theory by Wheeler holds not only for low dielectric substrates but also for the high dielectric substrates as well.

Yamashita and Mitra used their theory to study the microstrip wavelength. Figure 3.15 shows their curves on some low and high dielectric substrates.

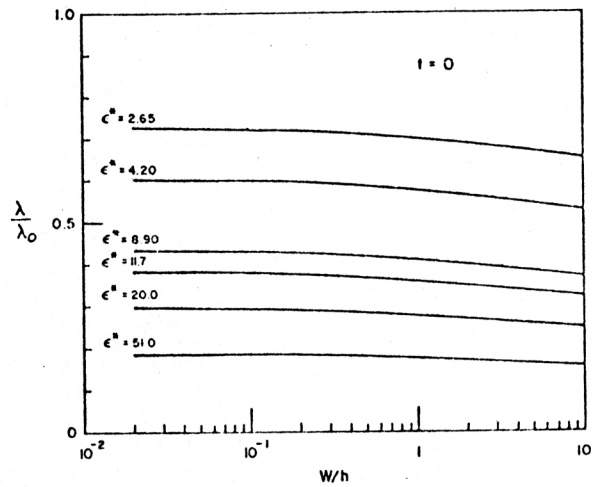

Fig. 3.15. Guide wavelength versus strip width and strip height.

From Figs. 3.14 and 3.15, it is clear that the microstrip wavelength is always less than the free space wavelength. For low (w/h) the microstrip wavelength is seen to be nearly independent of w/h for any given value of dielectric constant.

Propagation Velocity. The propagation velocity on microstrip differs from that of light if the dielectric used is not air. It is always less than the velocity of light.

The microstrip velocity calculations were based on capacitance calculations and measurements.

Bryant and Weiss (21) plotted the velocity versus the microstrip geometry (w/h) for different dielectric constants. Figure 3.16 shows their curves.

It is clear from Fig. 3.16 that when the dielectric constant is unity, the velocity is that of light and the propagation is TEM. The velocity becomes less than that of light when the dielectric constant of the substrate increases. Velocity is inversely proportional to the dielectric constant.

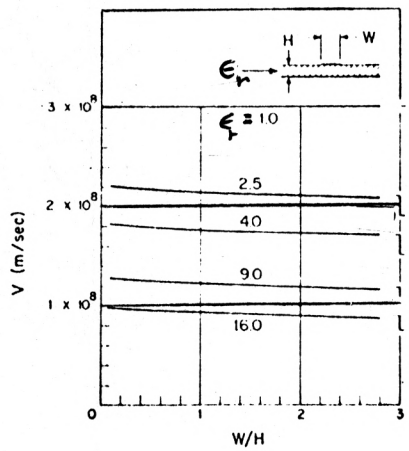

Fig. 3.16. Velocity of propagation on microstrip--single strip.

Judd and his colleagues (23) plotted the relative phase velocity of propagation to velocity of light on shielded microstrip versus the ratio (w/h). Figure 3.17 shows Judd's curves for $\epsilon_r = 9.8$ and $\epsilon_r = 9.3$.

Sobol's equations (3.6) may also be used to calculate the velocity of propagation on unshielded microstrip.

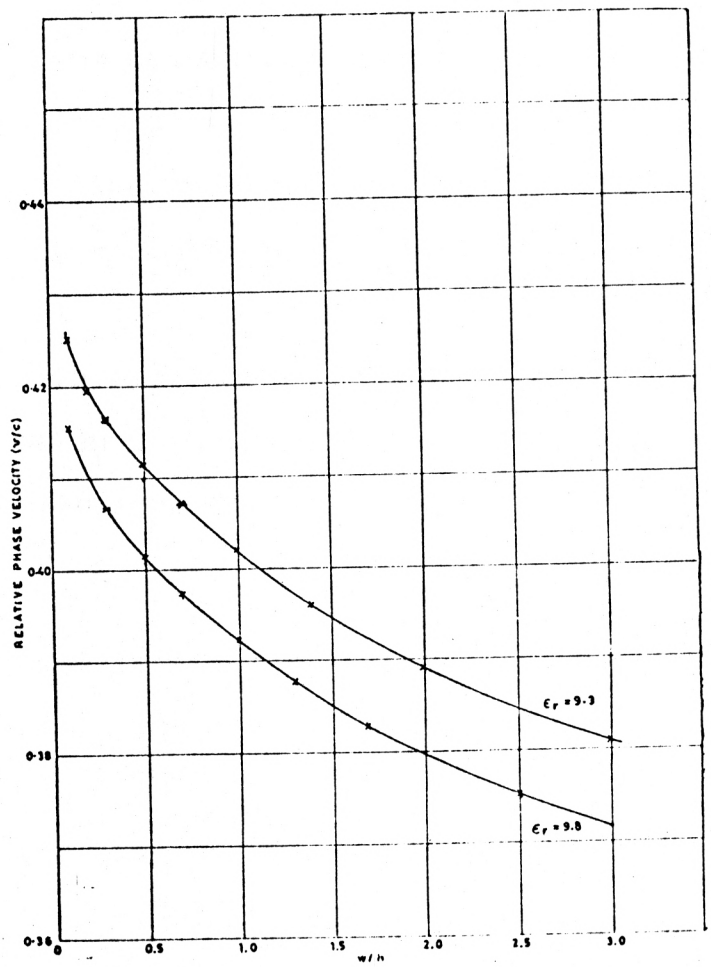

Fig. 3.17. Relative phase velocity of shielded microstrip.

CHAPTER IV

DISCONTINUITIES IN MICROSTRIP

The topic of discontinuity has not received much attention in the recent literature. Arditi (4) studied some microstrip discontinuities and discovered some very important properties which will be discussed in this chapter.

Every discontinuity radiates energy, and hence increases the total loss in microstrip. Radiation has been discussed in Chapter II.

Reflection is also one of the problems of discontinuities and has to be taken into account when designing any microstrip component that involves discontinuities.

4.1. Bends

It has been determined experimentally that reflection and radiation depend on the type of bend as well as the range of frequency.

Arditi found that the right-angle bend (Fig. 4.1a) gives maximum reflection. The 45-degree cut (Fig. 4.1b) and the smooth round corner (Fig. 4.1c) produce no appreciable reflection in the frequency band from 4 GHz to 5 GHz. The radiation loss is also very small in the case of the round corner.

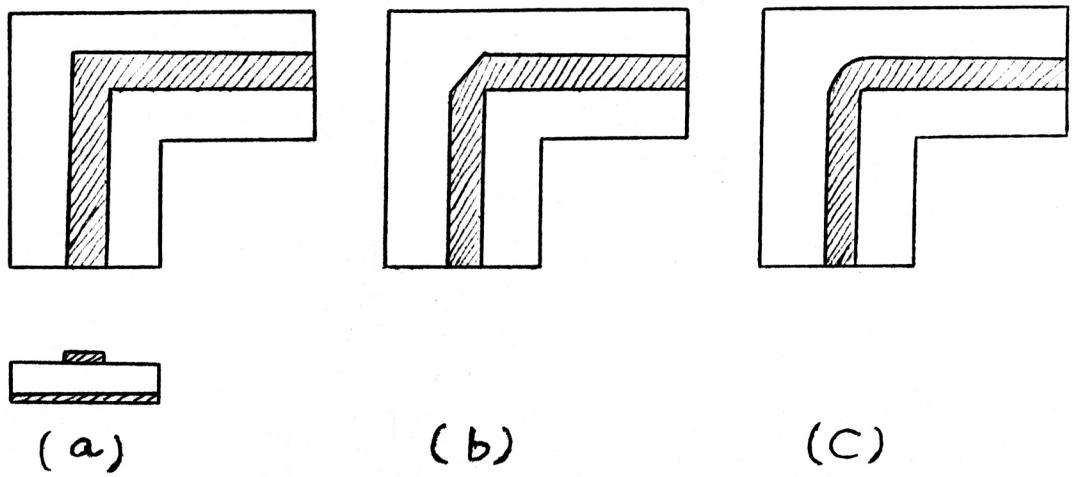

Fig. 4.1. Microstrip bends.

4.2. Step Discontinuity

Arditi showed that the equivalent circuit of a microstrip step discontinuity (Fig. 4.2) is an ideal transformer, provided the losses in the line are small.

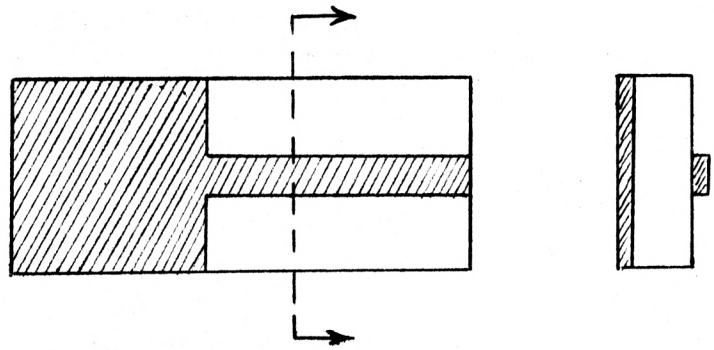

Fig. 4.2. Step discontinuity.

Figure 4.3 shows the variation of N^2, the square of the turns ratio of the equivalent transformer, as it varies with the line width (4). No one, to our knowledge, has studied the microstrip transformer since Arditi in 1953 introduced the idea of step discontinuity.

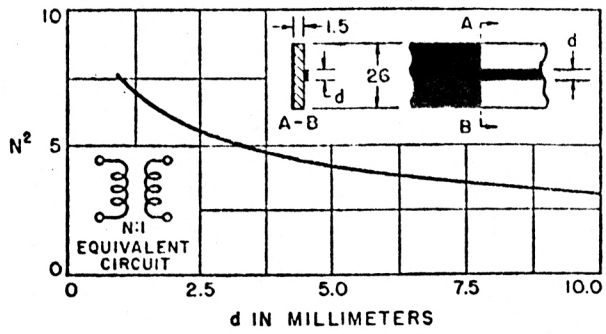

Fig. 4.3. Microstrip step discontinuity and equivalent transformer circuit. In the equivalent circuit, the reference plane is at AB. The dimensions are given in millimeters. The frequency is 4700 megacycles.

4.3. Gaps or Slots in Microstrip

The concept of scattering coefficients in microstrip is similar to that in waveguides. Let the incident and reflected waves be normalized as follows:

$$a_n = \frac{V_{n+}}{\sqrt{Z_{on}}}$$

$$b_n = \frac{V_{n-}}{\sqrt{Z_{on}}} \qquad (4.1)$$

where a_n is the incident wave and b_n is the reflected wave. V_{n+} is the voltage at the input and output of the wave going into the system, Fig. 4.4. V_{n-} is the voltage, at both terminals of the microstrip, of the wave going out of the system, and n is the terminal number.

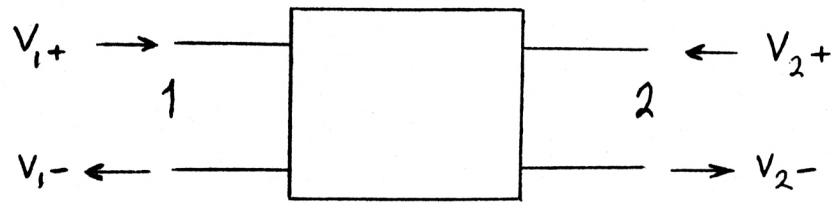

Fig. 4.4. Incident and reflected waves at ports of microstrip network.

$$V_n = V_{n+} + V_{n-} = \sqrt{Z_{on}}\,(a_n + b_n)$$

$$I_n = \frac{1}{Z_{on}}(V_{n+} - V_{n-}) = \frac{1}{\sqrt{Z_{on}}}(a_n - b_n) \qquad (4.2)$$

The average power flowing into the terminal is given by

$$[W_n]_{av} = \frac{1}{2}\,\mathrm{Re}(V_n I_n^*)$$

$$= \frac{1}{2}\,\mathrm{Re}\left[(a_n a_n^* - b_n b_n^*) + (b_n a_n^* - b_n^* a_n)\right] .$$

Since a complex quantity minus its conjugate is imaginary, then the average power going into terminal n is given by:

$$[W_n]_{av} = \frac{1}{2}\,(a_n a_n^* - b_n b_n^*) \qquad (4.3)$$

The incident and reflected waves in terminals 1 and 2 are related (26) by the expression:

$$b_1 = S_{11}\, a_1 + S_{12}\, a_2$$

$$b_2 = S_{21}\, a_1 + S_{22}\, a_2 \qquad (4.4)$$

The coefficients S_{11}, S_{12}, S_{21}, and S_{22} are called the scattering coefficients of the microstrip. The above equation may be written in matrix form.

$$\begin{bmatrix} b_1 \\ b_2 \end{bmatrix} = \begin{bmatrix} S_{11} & S_{12} \\ S_{21} & S_{22} \end{bmatrix} \begin{bmatrix} a_1 \\ a_2 \end{bmatrix} \qquad (4.5)$$

or $$[b] = [S][a]$$

$[S]$ is the scattering matrix. If terminal 2, the output, is connected to a matched load $a_2 = 0$, then

$$b_1 = S_{11}\, a_1$$

$$b_2 = S_{21}\, a_1 \qquad (4.6)$$

Thus S_{11} may be defined as the input reflection coefficient, in magnitude and phase, when the output is matched. S_{12} $(= S_{21})$ is defined as the ratio of reflected wave at the output and incident wave at the input, when the output is matched. S_{12} is always complex and its amplitude squared, $|S_{12}|^2$, is called the transmission coefficient.

It has been found by Arditi that for a given gap spacing, the values of the reflection coefficients are a function of the angle of the slot in the strip line (Fig. 4.5).

Figure 4.6 shows the variation of the transmission coefficient $|S_{12}|^2$, as defined before, with the gap spacing (d).

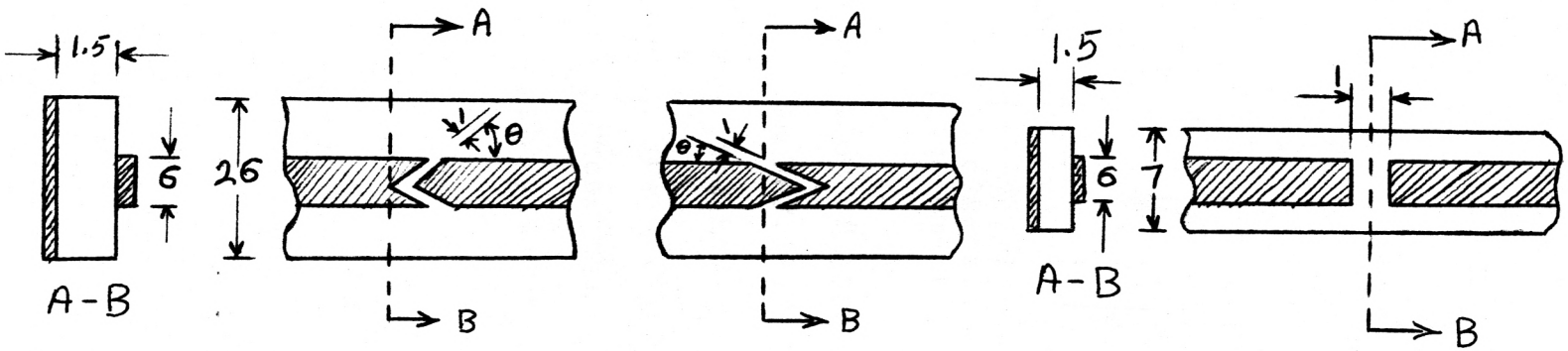

Scattering matrix coefficients (reference plane at AB)

θ = 17 degrees	S_{11}=-0.35-j0.68 $\pm S_{12}$=-0.53+j0.29 S_{22}=-0.28-j0.68	θ = 40 degrees	S_{11}=0.72-j0.65 $\pm S_{12}$=0.08+j0.24 S_{22}=0.96+j0.12
θ = 45 degrees	S_{11}=0.45-j0.86 $\pm S_{12}$=0.06+j0.29 S_{22}=0.59+j0.70	θ = 90 degrees	S_{11}=0.98-j0.12 $\pm S_{12}$=0.03+j0.20 S_{22}=0.93-j0.10

Fig. 4.5. Gaps in microstrip. The dimensions are in millimeters. The measurement frequency is 4700 megacycles.

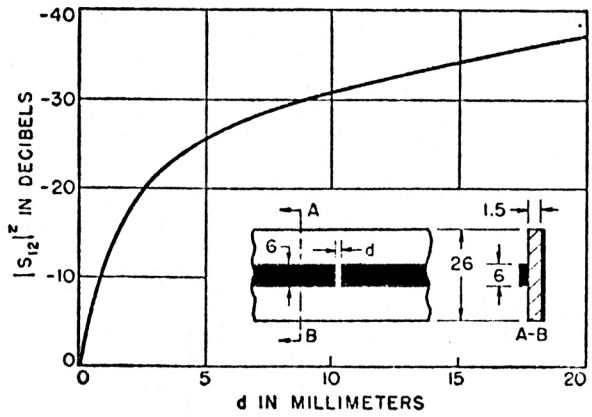

Fig. 4.6. Gaps in microstrip--transmission coefficient. The dimensions are in millimeters. The measurement frequency is 4700 megacycles.

The variation of gap capacitance with gap spacing is shown in Fig. 4.7 (see Ref. 27). Knowing d, the capacitance can be obtained for a line having w = 20 mils, $\epsilon_r = 8.875$, and $Z_o = 50$ ohms at 2 GHz. The difference shielding makes is clear from Fig. 4.7; it reduces the capacitance because it increases the amount of coupling, due to the reduction of radiation loss.

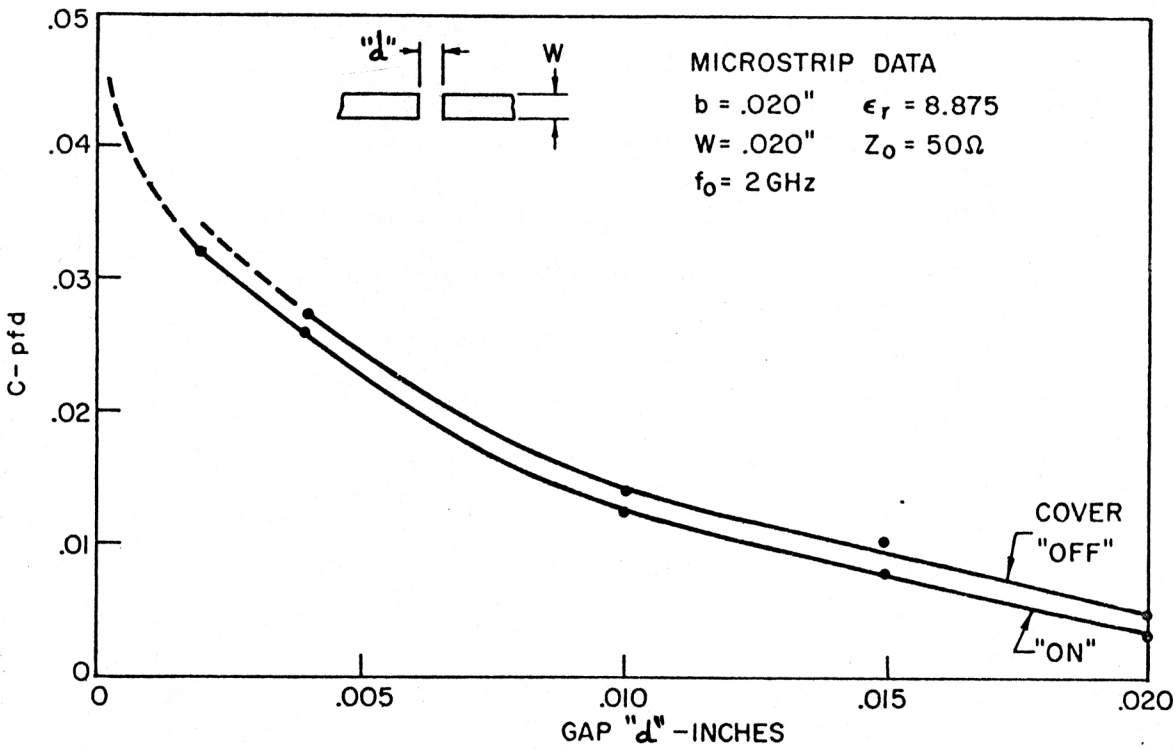

Fig. 4.7. Gap capacitance versus gap spacing.

CHAPTER V

MICROSTRIP COMPONENTS

Microstrip components are widely used in microwave technology today because they are easily fabricated by printed circuit techniques. They possess undoubted economic and technical merits. This chapter is devoted to the study of some microstrip components such as directional couplers, and resonant sections. The idea of coupling will be discussed in the first section to provide some basis to the study of directional couplers and resonant sections. Microstrip filters will not be studied here because of the large amount of network synthesis material which would have to be included to make the study meaningful. It is, in fact, a good topic for a separate report.

5.1. Coupling of Microstrip Lines

The idea of coupling has been well known for a long time, such as coupling between different kinds of transmission lines and waveguides. It has been found that coupling between microstrip lines leads to very important phenomena and some microstrip components have been made from coupled lines such as directional couplers, magic T's, hybrids, and filters.

Coupling may be in parallel, that is, the lines are printed with some portions parallel to each other, or in series, where gaps are made in the lines to form some sort of discontinuity.

The latter was discussed in the last chapter. Susceptances may be produced by parallel coupled junctions but the value of susceptance is limited because of quality factor considerations. In the design of high Q resonant sections one should consider the radiation problem. It is radiation from the ends of the lines which limits the use of parallel coupled junctions as high Q resonant sections. Figure 5.1 shows several configurations together with the corresponding values of the scattering matrix coefficients measured by Arditi.

Bryant and Weiss (21) studied the characteristics of coupled pairs of microstrip lines. They discovered that the normal modes of propagation on a pair of parallel strips of equal dimensions have even and odd symmetry with respect to reflection. They also found that in the quasi-static limit, where propagation is approximately TEM, the characteristic impedances of the two modes can be determined from their respective d-c capacitances and low frequency velocities. The difference in impedances becomes large as the coupling between the strips is increased by reducing the spacing (S) between them.

The physical construction of a coupled pair of microstrip lines is shown in Fig. 5.2. The configuration is conventionally specified by the parameters (w/h) and (s/h) together with ϵ_r, the relative dielectric constant of the substrate.

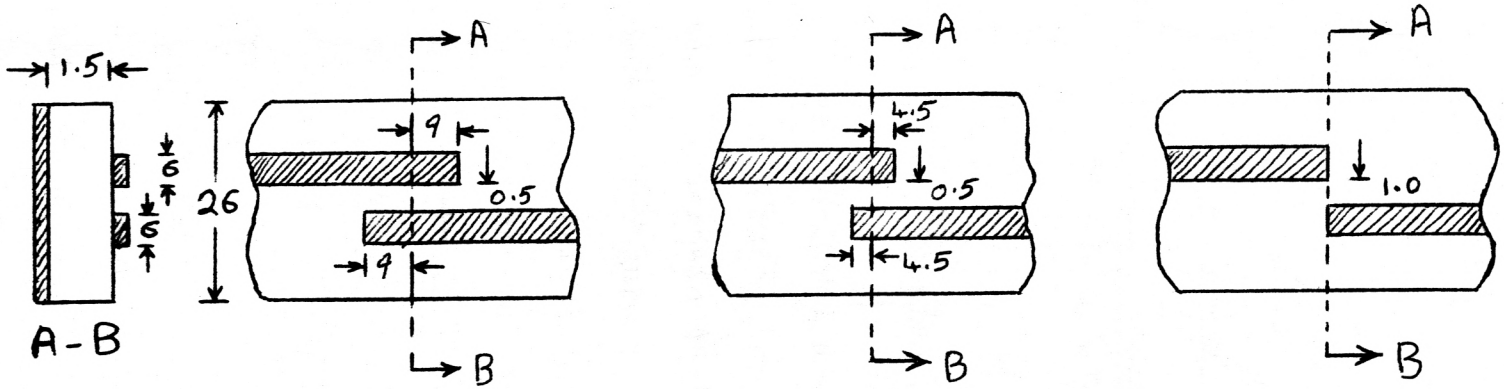

Scattering matrix coefficients (reference plane at AB)

$S_{11} = -0.95 - j0.09$	$S_{11} = -0.93j$	$S_{11} = 0.95$
$\pm S_{12} = 0.07 - j0.19$	$\pm S_{12} = 0.36$	$\pm S_{12} = 0.30j$
$S_{22} = -0.94 - j0.09$	$S_{22} = -0.89j$	$S_{22} = 0.90$

Fig. 5.1. Microstrip parallel coupled junctions. All dimensions are given in millimeters. The frequency is 4700 megacycles.

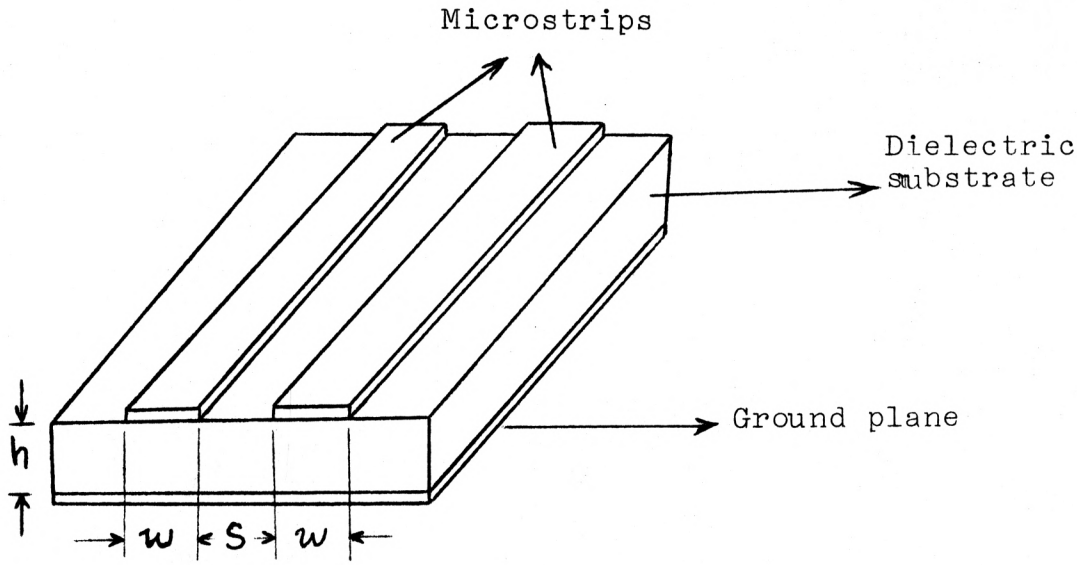

Fig. 5.2. Coupled pair of microstrip transmission lines.

Design curves are available in microwave handbooks from which the spacing (s) between microstrip lines can be calculated for certain desired values of coupling and characteristic impedance. Figure 5.3 shows the variation of (w/h) with (s/h) for a dielectric that has $\epsilon_r = 8.875$. One curve is plotted on the assumption that the conductor thickness is zero and the other when the thickness of the conductor is appreciable compared to that of the dielectric t/h = 0.025. Figure 5.4 shows the coupling in decibels as plotted against (s/h) for the same material.

For a given dielectric constant and substrate thickness, and a particular desired characteristic impedance, the line width can be calculated from characteristic impedance design curves such as Fig. 2.3. Once the line width (w) is calculated,

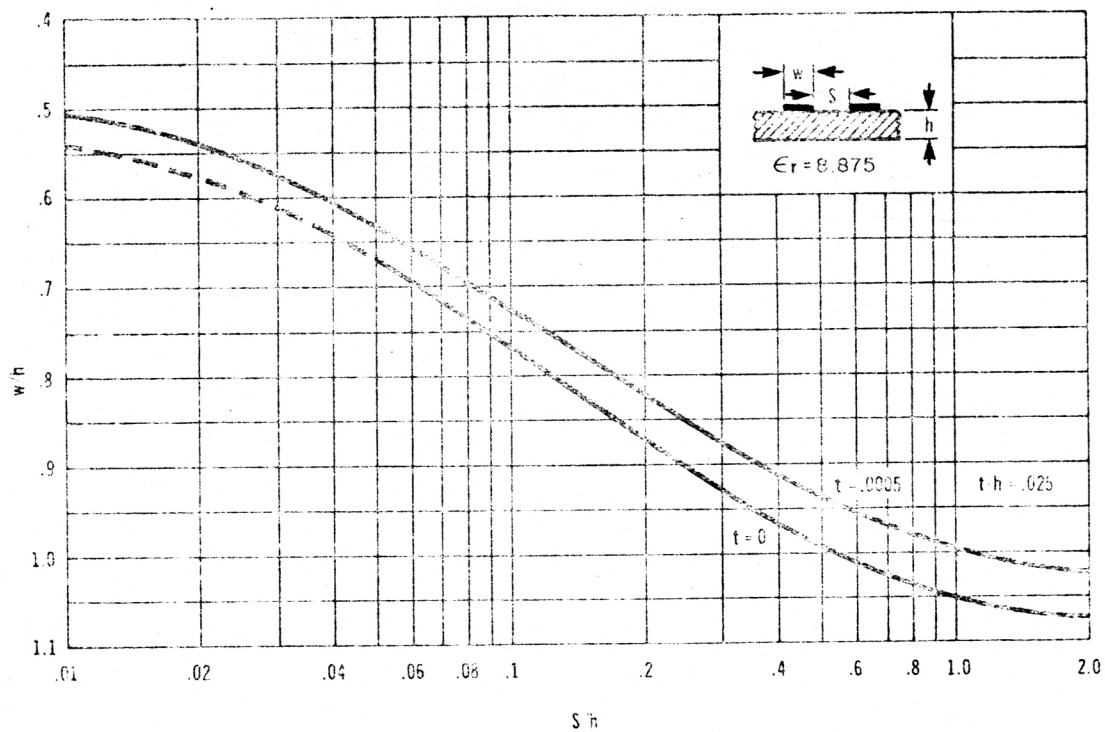

Fig. 5.3. (w/h) versus (s/h).

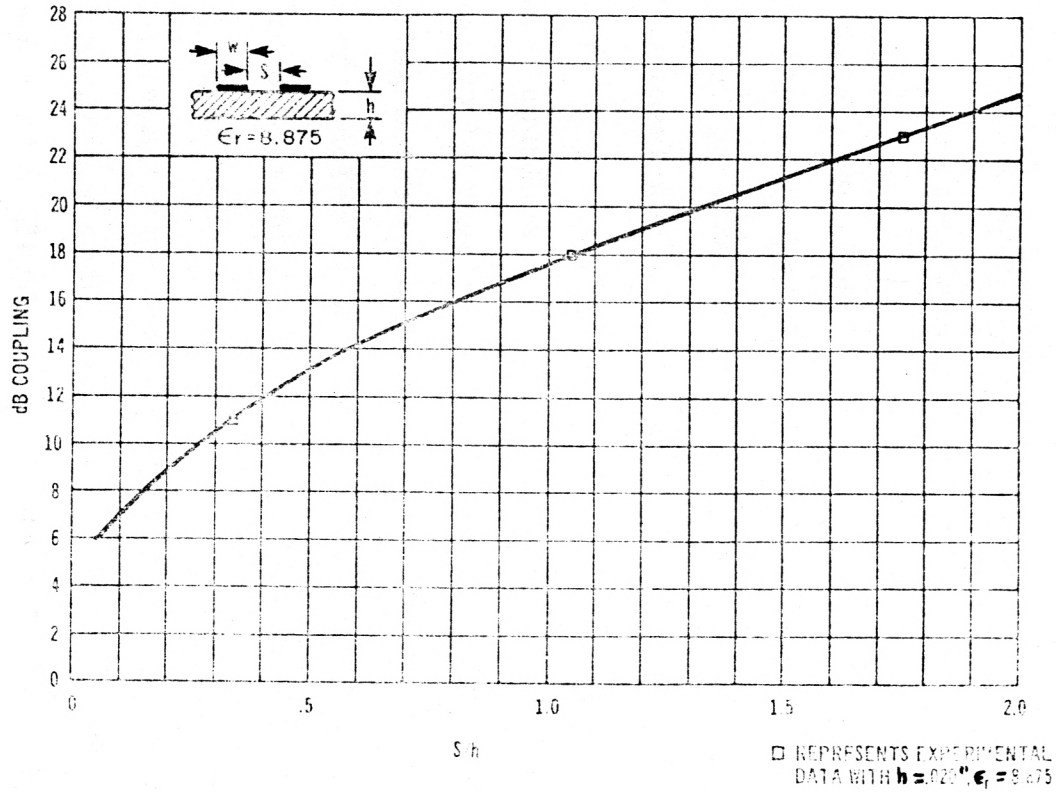

Fig. 5.4. Microstrip coupling versus (s/h).

and (w/h) is known, the ratio (s/h) may be found from Fig. 5.3. Knowing (s/h), the separation between microstrip lines (s) may be found. The coupling can be easily obtained from Fig. 5.4 since (s/h) is known. Therefore for a certain characteristic impedance the line width and the separation between lines are found from the design curves. The value of coupling in decibels is also obtainable from curves.

5.2. Directional Couplers

The principle of operation of microstrip couplers is identical to that of parallel coupled waveguides. When the coupling interval is several wavelengths long, broadband directivity can be achieved.

Microwave couplers in microstrip may be formed by placing the two lines to be coupled close to each other or by providing direct coupling between the lines at two or more points. This latter kind of coupler is widely used as a hybrid coupler because it is easier to get 3-dB coupling than in the case of the parallel lines coupler which will be described here.

The performance of directional couplers in general is specified in terms of the coupling factor and the directivity. The coupling factor of a microstrip directional coupler is defined in decibels as:

$$\text{Microstrip coupling factor} = 10 \log_{10} \frac{P_1}{P_4} \text{ dB} \qquad (5.1)$$

where P_1 is the power entering the microstrip line at port 1, Fig. 5.5, and P_4 is the power delivered, through coupling, to port 4. Ports 2 and 3 are connected to a matched load.

The line connecting ports 1 and 2 is called the main microstrip line and the line connecting ports 3 and 4 is called the auxiliary microstrip line.

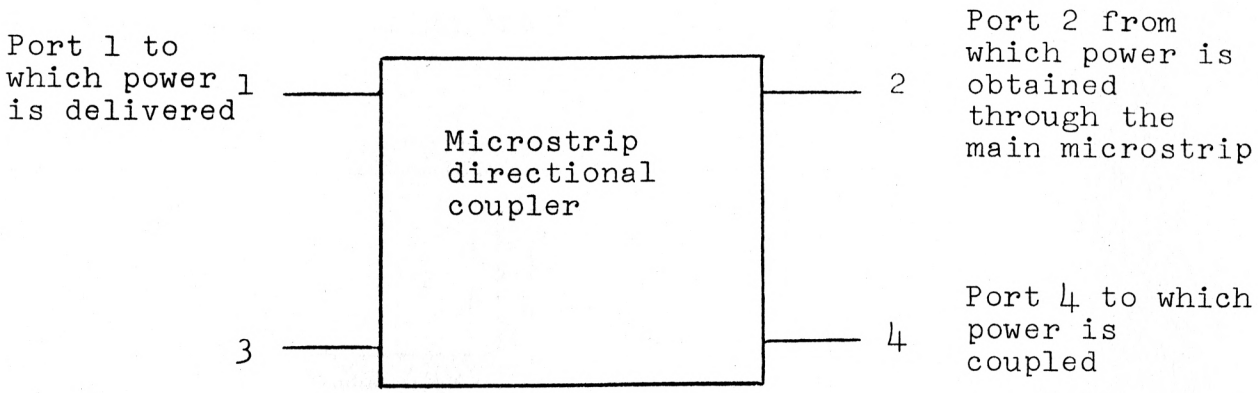

Fig. 5.5. Microstrip directional coupler.

The coupling factor is a measure of how much power is coupled from the main to the auxiliary microstrip lines.

Directivity is defined as:

$$\text{Directivity} = 10 \log_{10} \frac{P_4}{P_3} \text{ dB} \qquad (5.2)$$

It indicates how well the forward wave in the main microstrip is coupled only to the desired port in the auxiliary microstrip. It is desired to have P_3 as close to zero as possible. In a well designed microstrip directional coupler P_3 is very small.

If power enters port 3, the line connecting ports 3 and 4 is the main microstrip line, and it will deliver power to ports 2 and 4 and a negligible amount of power will appear in port 1. This statement follows because of reciprocity.

It has been assumed that there are no reflections; the lines are smooth with no discontinuities. If these assumptions are not valid, outputs will appear in all the ports and reflections may be found using the above mentioned technique.

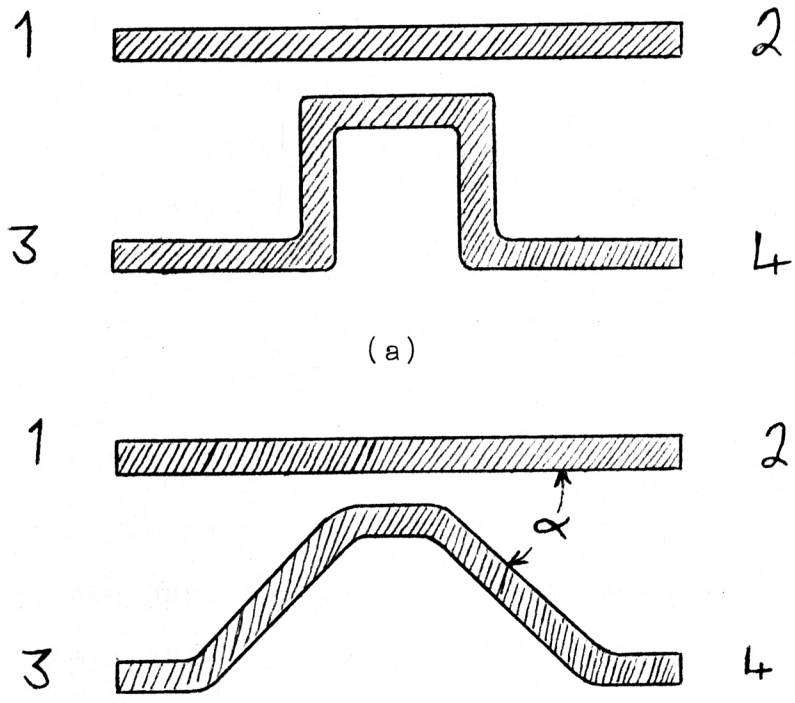

Fig. 5.6. Microstrip directional couplers.

Figure 5.6 shows the kind of directional coupler tested by Arditi and found to be excellent for microwave use. The directivity is very high and the coupling is good. Ports 2 and 4 are found to receive about equal power, and port 3 a very small amount of power. Arditi, from his experimental work, found that the directivity and coupling are functions of the angle of approach (α) of one line with respect to the other.

When α is 90 degrees, Fig. 5.6a, the coupling is not very good and the directivity is not high. When α is 30 degrees, good coupling and high directivity are achieved.

For α less than 30 degrees, the coupler can be used as a broadband magic T. Effectively, in that case, when all arms of the coupler are connected to matched loads, terminals 2 and 4 will receive an almost equal amount of power from the input signal source at 1 and terminal 3 will receive an amount of power about 30 dB below those of 2 or 4. Moreover, it has been observed by Arditi that these properties apply almost equally well when any of the terminals 1, 2, 3, or 4 is taken as the input.

Bowness (5) studied the same kind of directional coupler and found it quite satisfactory. He studied in particular the factors (s), the separation of the lines, and (L) the length over which the separation is maintained (Fig. 5.7). He also

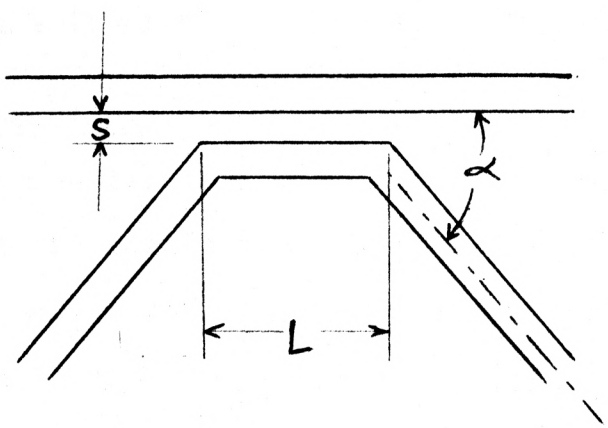

Fig. 5.7. Microstrip directive coupler.

investigated the effect of the angle of approach and found that the directivity depends mainly on this angle (α) and that the smaller the angle, the greater the directivity and vice versa, up to about 90 degrees.

Figure 5.8 shows Bowness' results for the variation of coupling with (L), the coupling interval. The curves must be asymptotic to the L = 0 axis and to the line giving a coupling of -3 dB because if the length L is great enough, the lines will share the power equally. The graph indicates that the greater the angle, the more critical is the length for small coupling. Increasing the separation (s) will reduce the coupling.

There is another type of coupler shown in Fig. 5.9 in which the coupling depends on the width (d). The separation between the lines should be a quarter wavelength in this kind of coupler. This kind of coupler is useful if less than -10 dB is required. By varying the width (d), a coupling of -3 dB may be obtained. This is effectively a microwave hybrid coupler.

5.3. Resonant Sections

It has been mentioned when dealing with discontinuities, Chapter IV, that the parallel and series coupled junctions realize susceptances. By placing two such discontinuities at the proper distance apart, a resonant section can be obtained.

The length of the coupling sections makes the composite junction frequency dependent, and hence produces a resonant section useful as a filter element.

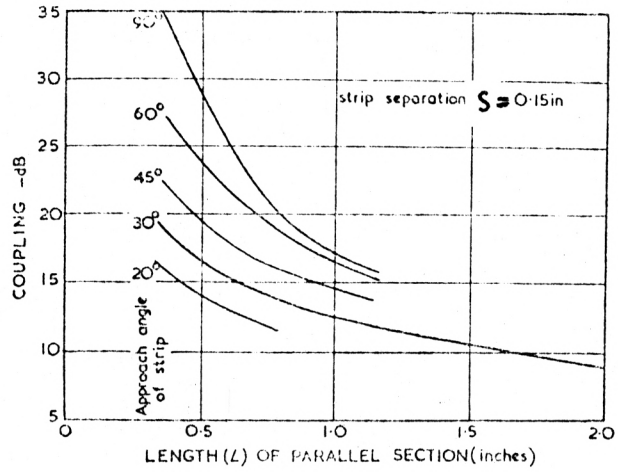

Fig. 5.8. Coupling as varied with (L).

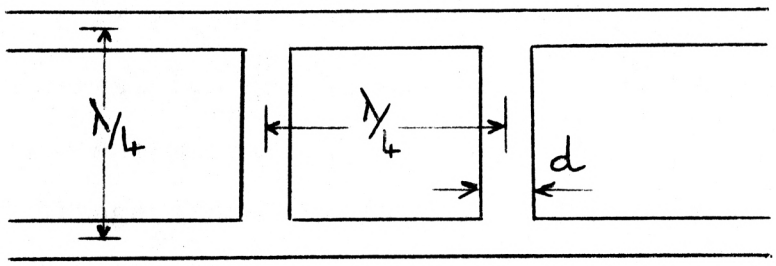

Fig. 5.9. 3-dB coupler.

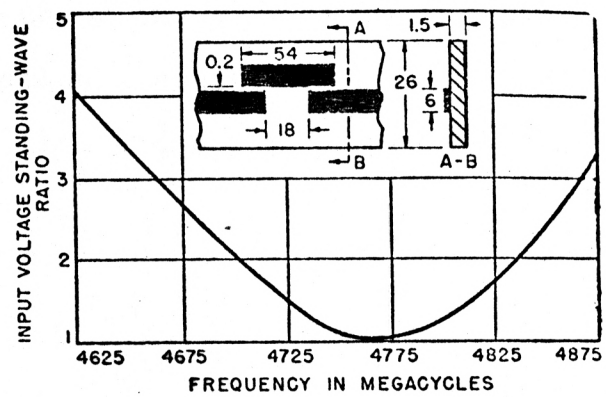

Fig. 5.10. Microstrip resonant section with parallel coupled junctions. All dimensions are given in millimeters. The insertion losses at center frequency were 0.8 decibel.

Arditi (4) tested some resonant sections and plotted the input voltage standing wave ratio versus frequency. He obtained a resonant curve for each section.

Figure 5.10 shows a resonant curve of a parallel coupled section with a resonant frequency of about 4.763 GHz. The length of the coupling interval of 54 millimeters is less than the resonant wavelength (about 63 mm). At the resonant frequency the input voltage standing wave is unity and increases above and below this frequency.

Figure 5.11 is Arditi's resonant curve of a series coupled section. The resonant frequency is the same as that of the parallel coupled section, Fig. 5.10, but the length of the coupling interval (68 mm) is different. It is here greater than the resonant wavelength (63 mm). At the resonant frequency the input voltage standing wave ratio is about 1.4.

From Figs. 5.10 and 5.11 it is clear that the resonance obtained with the series section is better as far as the selectivity is concerned but this is due to the insertion loss being more in the case of the section with gaps.

The radiation losses from the discontinuities and the losses in the line are a limitation in obtaining higher Q values.

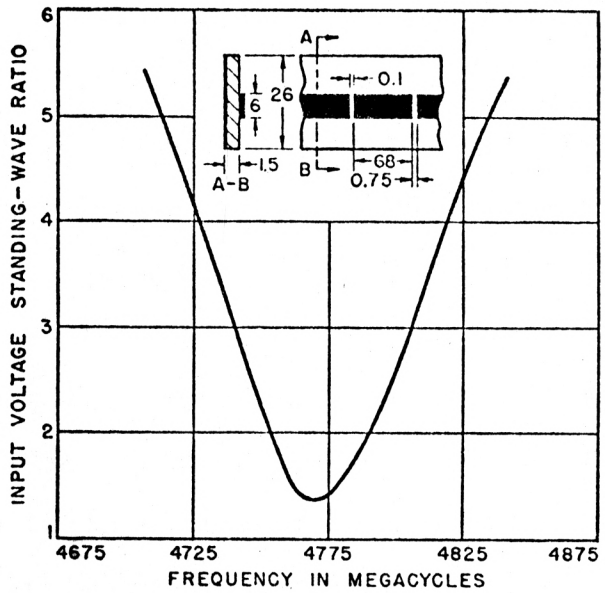

Fig. 5.11. Microstrip resonant section with gaps in the line. All dimensions are in millimeters. The insertion losses at center frequency were 6.5 decibels.

CHAPTER VI

SUMMARY AND CONCLUSION

Microstrip transmission line theory, characteristics, some discontinuities, and some components are studied in this report to provide a small text that includes the main formulas and design curves developed so far. The report dealt only with microstrip lines printed on nonmagnetic substrates of low and high dielectric constant. In Chapter I, the transmission mode is discussed; TEM is found to be a good approximation giving close results to those measured by several workers.

In Chapter II the general theory of microstrip is considered. The width of the strip line tends to have an effective value equal to the actual width plus an incremental width given by equation (2.2). The quality factor of microstrip is also considered in the general theory. Losses are studied in a separate section in Chapter II. Equations for the dielectric and conductor losses are derived. The effective dielectric constant of microstrip is studied and its dependence on several factors is discussed. Radiation as one of the problems of microstrip is discussed in section 2.3 and an equation for the radiation resistance of microstrip is given, equation (2.7).

In Chapter III, the characteristic impedance is explored and some useful design curves are given. Shielding and its

effect upon the characteristics of microstrip are considered. The propagation wavelength and velocity are studied in some detail. Design equations and curves for the propagation wavelength are given for reference.

Chapter IV is devoted to the consideration of some of the discontinuities experimentally studied, mostly by Arditi (4). The dependence of the scattering coefficients on the angle of approach and the gap spacing is also considered for different kinds of discontinuity.

Coupling between microstrip lines, directional couplers, and resonant sections are treated in Chapter V to provide some information about microstrip components and their use in the microwave frequency range.

It is concluded that the use of this transmission technique with integrally formed semiconductor devices provides the opportunity for simpler, less expensive microwave components of improved performance.

Transition between microstrip components and coaxial cables is easy using the commercially available transition devices.

Microstrip transmission line is in use in the modern microwave technology (13, 20). It has been proved that microstrip components possess undoubted technical and economic merits.

REFERENCES

1. D. D. Grieg and H. F. Engelmann, "Microstrip--a new transmission technique for the kilomegacycle range." Proc. IRE, vol. 40, December, 1952, pp. 1644-1650.

2. F. Assadourian and E. Rimai, "Simplified theory of microstrip transmission system." Proc. IRE, vol. 40, December, 1952, pp. 1651-1657.

3. J. A. Kostriza, "Microstrip components." Proc. IRE, vol. 40, December, 1952, pp. 1658-1663.

4. M. Arditi, "Experimental determination of the properties of microstrip components." Electrical Communication, December, 1953, pp. 283-293.

5. C. Bowness, "Strip transmission lines," Electronic Engineering (London), January, 1956, pp. 2-7.

6. J. M. Dukes, "An investigation into some fundamental properties of strip transmission lines with the aid of an electrolytic tank." Proc. IEE, vol. 103, pt. B, May, 1956, pp. 319-333.

7. T. T. Wu, "Theory of the microstrip." Journal of Applied Physics, vol. 28, March, 1957, pp. 299-302.

8. J. M. Dukes, "The application of printed circuit techniques to the design of microwave components." Proc. IEE, vol. 105, pt. B, March, 1958, pp. 155-172.

9. H. A. Wheeler, "Transmission line properties of parallel wide strips by a conformal-mapping approximation." IEEE Trans. on MTT, May, 1964, pp. 280-289.

10. H. A. Wheeler, "Transmission line properties of parallel strips separated by a dielectric sheet." IEEE Trans. on MTT, March, 1965, pp. 172-185.

11. T. M. Hyltin, "Microstrip transmission on semiconductor dielectrics." IEEE Trans. on MTT, vol. 13, November, 1965, pp. 777-781.

12. M. Caulton, J. Hughes, and H. Sobol, "Measurements on the properties of microstrip transmission lines for microwave integrated circuits." RCA Review, September, 1966, pp. 377-391.

13. H. Sobol, "Extending IC technology to microwave equipment." Electronics, March 20, 1967, pp. 112-124.

14. G. D. Vendelin, "High dielectric substrates for microwave hybrid integrated circuitry." IEEE Trans. on MTT, December, 1967, pp. 750-752.

15. R. Seckelmann, "On measurements of microstrip properties." The Microwave Journal, January, 1968.

16. P. Silvester, "TEM wave properties of microstrip transmission lines." Proc. IEE, vol. 115, January, 1968, pp. 43-48.

17. E. Yamashita and R. Mitra, "Variational method for the Analysis of microstrip lines." IEEE Trans. on MTT, vol. 16, April, 1968, pp. 251-256.

18. R. Pucel, D. Masse', and C. Hartwig, "Losses in microstrip." IEEE Trans. on MTT, vol. 16, June, 1968, pp. 342-350.

19. R. Pucel, D. Masse', and C. Hartwig, "Correction to losses in microstrip." IEEE Trans. on MTT, December, 1968, p. 1064.

20. E. W. Matthews and R. M. Rector, "Hybrid techniques at microwave frequencies." Hybrid Micro-electronics Symposium, October, 1968, pp. 439-449.

21. T. G. Bryant and J. A. Weiss, "Parameters of microstrip transmission lines and a coupled pairs of microstrip lines." IEEE Trans. on MTT, vol. 16, December, 1968, pp. 1021-1027.

22. E. J. Denlinger, "Radiation from microstrip resonators." IEEE Trans. on MTT, vol. 17, April, 1969, pp. 235-236.

23. S. Judd, R. Clowes, and D. Rickard, "An analytical method for calculating microstrip transmission line parameters." IEEE Trans. on MTT, vol. 18, February, 1970, pp. 78-87.

24. M. K. Krage and G. I. Haddad, "Characteristics of coupled microstrip transmission lines," I and II. IEEE Trans. on MTT, vol. 18, April, 1970, pp. 217-228.

25. W. J. Chudobiak, P. P. Jain, and V. Makios, "Dispersion in microstrip." IEEE Trans. on MTT, vol. 19, September, 1971, pp. 783-784.

26. S. Ramo, J. Whinnery, and T. Van Duzer, "Fields and waves in communication electronics." John Wiley and Sons, Inc., New York, N. Y., 1965.

27. T. S. Saad, "Microwave engineers handbook," Vol. 1. Artech House, Inc., Bedham, Mass., 1971.

ACKNOWLEDGMENT

I wish to express my appreciation to Dr. Gary Johnson, my major professor, and acknowledge with gratitude his numerous helpful suggestions and comments. I also thank Dr. Kendall Casey and Dr. Said Ashour for their suggestions and assistance in maintaining consistency and accuracy in the manuscript. My thanks to Dr. D. R. Hummels, the chairman of my committee, for his help, and to Dr. M. S. Lucas for providing me with the equipment and material to build some microstrip components.

Finally, I owe a special debt of gratitude to the University of Libya for sponsoring my graduate study and providing me with financial support.

MICROSTRIP TRANSMISSION LINE THEORY, CHARACTERISTICS, AND COMPONENTS

by

MOHAMED A. USTA

B.Sc. (Electrical Engineering),
University of Libya, 1969

AN ABSTRACT OF A MASTER'S REPORT

submitted in partial fulfillment of the

requirements for the degree

MASTER OF SCIENCE

Department of Electrical Engineering

KANSAS STATE UNIVERSITY
Manhattan, Kansas

1972

This report deals only with microstrip lines and components printed on nonmagnetic substrates of low and high dielectric constant, and provides a text that includes the design equations and curves for straight microstrip lines as well as qualitative information on line discontinuities and components.

The microstrip transmission line mode of propagation, which is quasi-TEM, is discussed. The effective width of microstrip line is described and its equation is derived from Wheeler's theory. The loss theory of Pucel is studied and formulas for the dielectric and conductor losses are derived. Pucel and Coulton's curves for the conductor loss as a function of w/h, the line width to dielectric thickness ratio, are presented and discussed. The quality factor Q is considered and its formula as well as a curve showing how it depends on w/h are given. Radiation is described and Lewin's formula for the radiation resistance as well as Denlinger's equation for the radiated power are presented. Dispersion is considered and formulas for the effective dielectric constant of microstrip are given. The characteristic impedance, the propagation wavelength, and velocity are studied. Their equations are given as well as several curves made by the workers in the field, such as Coulton, Sobol, Vendelin, Seckelmann, Yamashita, Mitra, Bryant, Weiss, Judd, and Kostriza. Some discontinuities are studied, such as bends, step discontinuity, and gaps or slots. Coupling between microstrip lines is considered as well as some parallel and series coupled junctions. Directional couplers and resonant sections in microstrip form are described.